







Advanced system for air diffusion in the private quarters of the astronauts on the International Space Station

Extended Abstract

Author

Matei-Razvan GEORGESCU

Co-directors:

Prof. Dr. Ing. Amina MESLEM

Conf. Dr. Ing. Ilinca NASTASE

June 2021

Scientific Contributions

Journals

- **M.R.** Georgescu, A. Meslem, I. Nastase, F. Bode, *Personalized ventilation solutions for reducing CO2 levels in the crew quarters of the International Space Station*, pending major revision in Build. Environ (2021).
- **M.R. Georgescu**, A. Meslem, I. Nastase, L. Tacutu, *An alternative air distribution solution for better environmental quality in the ISS crew quarters*, Accepted for publication Int. J. Vent. (2021).
- **M.R.** Georgescu, A. Meslem, I. Nastase, M. Sandu, *Numerical and experimental study of the International Space Station crew quarters ventilation*, J. Build. Engineering (2021) https://doi.org/10.1016/j.jobe.2021.102714.
- **M.R. Georgescu**, A. Meslem, I. Nastase, *Accumulation and spatial distribution of CO2 in the astronaut's crew quarters on the International Space Station*, Build. Environ. 185 (2020) 107278.

Conference Proceedings

Matei-Razvan Georgescu, Ilinca Nastase, Amina Meslem, Mihnea Sandu, Florin Bode. Design of a Small-Scale Experimental Model of the International Space Station Crew Quarters for a PIV Flow Field Study, E3S Web of Conferences, EDP Sciences, 2019, 111, pp.01045.

Matei-Razvan Georgescu, Amina Meslem, Ilinca Nastase, Mihnea Sandu, Florin Bode. *Experimental Study of Carbon Dioxide Accumulation on a Model of the Crew Quarters on the ISS*, 9th International Conference on Energy and Environment, 2019, Timisoara, Romania

Matei-Razvan Georgescu, Amina Meslem, Ilinca Nastase, Mihnea Sandu, Florin Bode. *Numerical Prediction of Carbon Dioxide Accumulation in the International Space Station Crew Quarters*, 9th International Conference on Energy and Environment, 2019, Timisoara, Romania

Florin Bode, **Matei-Razvan Georgescu**, Amina Meslem, Ilinca Nastase, Mihnea Sandu. *Numerical Study for the Improvement of the Ventilation System of the Crew Quarters on Board the International Space Station*, Roomvent & Ventilation 2018, 2018, Espoo, Finland

Charles Berville, **Matei-Răzvan Georgescu**, Ilinca Năstase. *Numerical study of the air distribution in the Crew Quarters on board of the International Space Station*, E3S Web of Conferences, EDP Sciences, 2019, 85, pp.02015.

George-Madalin Chitaru, **Matei-Razvan Georgescu**, Costin Ioan Cosoiu, Catalin Nae. *Numerical study of a particle-laden flow in a harsh environment testing facility* The 7th International Symposium on Computational Wind Engineering, 2018, Seoul, South Korea

Matei-Razvan Georgescu, George-Madalin Chitaru, Costin Ioan Cosoiu, Ionut Brinza, Catalin Nae. Numerical study of the secondary phase dispersion in a particle-laden flow 2017

International Conference on Energy and Environment (CIEM), Oct 2017, Bucharest, Romania. pp.394-398.

Matei-Razvan Georgescu, Alexandru Cezar Vladut, Costin Ioan Cosoiu, Andrei-Mugur Georgescu. *Numerical study of the flow inside a wind trapping system* 2017 International Conference on Energy and Environment (CIEM), Oct 2017, Bucharest, Romania. pp.330-334.

Introduction

The present thesis studies the ventilation system of the crew quarters (CQ) on the International Space Station (ISS) Harmony module. As the aerospace industry looks ahead to long-duration missions conducted far from Earth [1], difficult issues arise related to the management and effects of human exposure to CO₂. In imponderability, the natural flow of convective air due to temperature differences is virtually non-existent. In a confined space, in the absence of adequate ventilation, the carbon dioxide (CO₂) exhaled by an astronaut accumulates in "pockets" around the head [2,3], representing an asphyxiation hazard. Thus, all space vehicles rely on forced ventilation to combat the negative effects of imponderability [4]. Forced ventilation is insufficient in a closed environment such as the ISS, and so complementary equipment (part of the Environmental Control and Life Support System - ECLSS) is present [4,5], allowing the decomposition of CO₂ into water and inorganic compounds.

The CQ is a private space for the astronauts where they can rest and take care of personal activities during their leisure hours. Originally the astronauts slept in a common space designated for sleep and rest [4,6] and astronaut feedback indicated a greater need for privacy and personalization of their CQ. This lead to the design of a new kind of CQ that could accommodate the needs for privacy and personalization [6,7]. This design, which is the subject of the present thesis, was destined for the Harmony module aboard the ISS. Since this module was an addition to the module, their design needed to fit in the standard payload racks [6–8] that are sent from Earth to the ISS. Four CQ cabins were thus sent up and mounted on the ISS in 2008.

Since then, reports indicated that while crew satisfaction with the new CQ design is generally good [9], reports since then have shown that symptoms of light CO₂ intoxication are still reported by astronauts [4,10,11]. During the review process of the new CQ design several design concerns were highlighted related to its ventilation system [8,9], notably that alarms indicating insufficient flow rate through the CQ were triggered when the fan was set to its lowest speed due to dust accumulation in the ducts. At the same time, higher fan speed settings led to noise complaints [8,9]. Considering these two issues in the context of CO₂ intoxication reports, leads to an indication, that the astronauts would benefit from having a ventilation system with improved flow rates as long as acoustic discomfort is avoided.

This indication forms the basis of the present thesis which studies a new ventilation system for the CQ cabins aboard the ISS Harmony module, whose purpose is to reduce CO₂ concentration inside the CQ in the attempt to eliminate CO₂ intoxication issues while at the same time maintaining the required air flow rates with minimal acoustic impact. The following section of the introduction will present a detailed account of the current conditions aboard the ISS CQ and an outline of the new proposed ventilation system, whose study is divided in 4 stages (each covering an aspect of the proposed solution). These stages will have their own sections (1 through 4) dedicated to an in-depth presentation of their subject's current state of the art and how this is integrated into the proposal of the present thesis.

State of the art and proposed approaches

In order to improve upon the existing solution, it is necessary to first understand both the present solution and the conditions under which it operates. The CQ designed for the Harmony Module (Figure 1) has two main components [7,8]: (1) the cabin itself meaning the interior volume where the astronauts sleep and store their belongings; and (2) a removeable section containing the ventilation circuits and the door of the CQ, which the designers [7,8] named "Bump-out" (Figure 1). The exterior of the "Bump-out" also features the air intake and exhausts, drawing and exhausting air from/to the corridor of the Harmony Module.

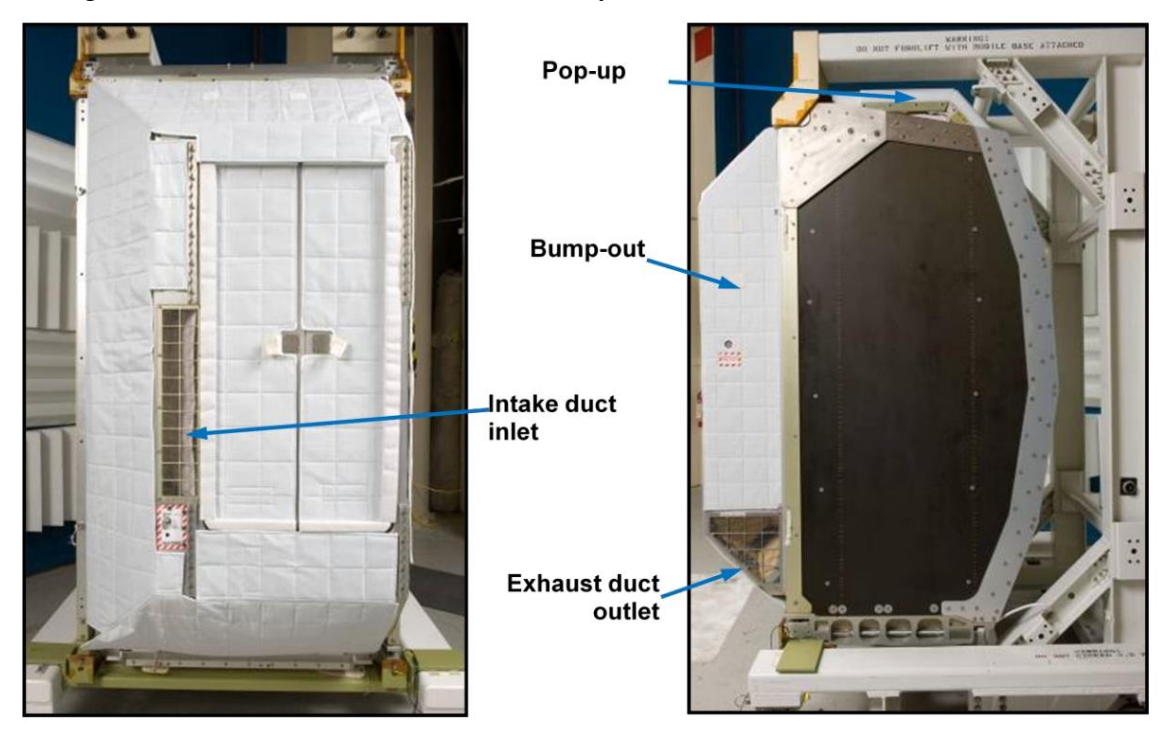


Figure 1 CQ front and side views highlighting the position of the intake and exhaust on the bump-out (Source: [8])

The ventilation system [8] is entirely situated within the "Bump-out" and is divided in two separate ventilation circuits: (1) the intake circuit (Figure 2a), and (2) the exhaust circuit (Figure 2a). The intake circuit (1) has an inlet which is situated to the left of the CQ door (Figure 1) and features an axial fan (Figure 2b) which directs air upwards through the ducts. The air following a sequence of turns and bends (Figure 2b) and is then directed through several channels separated by flow guide vanes (Figure 2b), finally exiting the circuit through the intake diffuser (Figure 2a). The exhaust circuit (2) has its inlet in the interior of the CQ, in the lower region of the "Bumpout" (Figure 2a). Air is absorbed by a second axial fan (Figure 2b) (identical to the intake fan) which directs the air towards the exhaust outlet which is seen on the lower right-side of the "Bumpout" (Figure 1).

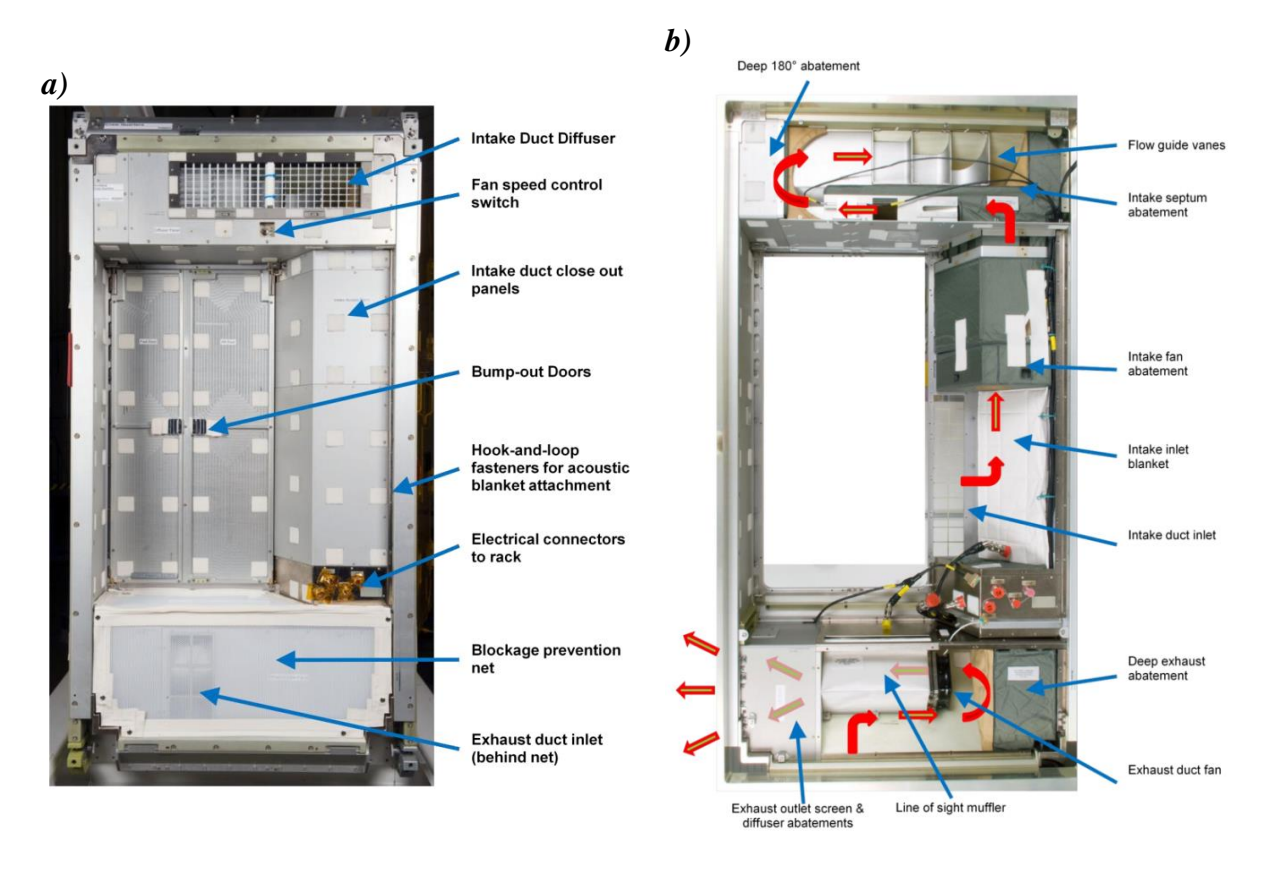


Figure 2 Bump-out interior view with the ducting covered (a) and with the ducts revealed (b) (Source: [8])

The ventilation circuits are complex, featuring multiple bends and turns. The explanation for this design is that when choosing fans for the ISS it is important that they are able to provide adequate flow rates while using as little power as possible [7,8,12] due to the limited energy supply of the ISS. Two axial fans were chosen for this purpose [7,8] (EBM Pabst 4184 NXH) for their low power consumption, good reliability, low acoustic signature and good flow parameters. Although the low acoustic signature was chosen out of necessity (recalling the noise complaints [8,9]) it was not sufficient. The ventilation ducts were lined internally with soundproofing material. The intricate geometry of the air introduction circuit (two elbows of 90° and 180° respectively along with the guiding vanes) also has a primary role in the dissipation of the noise coming through the ducting from the ISS corridor (background noise) and from the axial fans themselves [7,8]. It is worth noting that the interior surface of the CQ walls is covered with several layers of soundproofing materials (a Kevlar® wool pad with white Gore-Tex®, and Nomex® assembled in a quilted structure) that serve to mitigate the propagation of acoustic waves through the walls of the cabin structure [8].

The ventilation system parameters, of the CQ, have been pre-measured and estimated on Earth, previous to their deployment to the ISS [8,12]. The corresponding air flow rate interval is 96 - 162 m³/h (between 40-80 hourly air exchanges). For practical safety and maintenance purposes, the controller of the ventilation system allows the fans to operate at three different speeds corresponding to three values of the volumetric flow rate, respectively: 108, 138 and 156 m³/h. The fans are powered via a 24V direct current connection, with the previously mentioned three-step speed control configuration (low, medium, high) [7]. The measurements on Earth concluded

that the two thirds of the inner volume displays average velocity values between 0.051-0.23 m/s (a requirement for spacecraft which will be explained in the following paragraphs), and the noise level exceeds the NC-40 curve by 3-5 dB at frequencies between 250 - 750 Hz [8,12]. However, one must note here that the velocity values were probably obtained using a punctual portable thermo-anemometer that is typically employed for indoor climate assessment in buildings [8] and velocity distributions in the cabin volume are not available.

The CQ was designed to meet ISS airflow and acoustic environmental requirements [4,9,12]. The design document used [4] to obtain these requirements concerns spacecraft in general and human health aboard them and as such uses certain parameters to describe the atmosphere which are better suited for medicine than the built environment (for example giving concentration in terms of partial pressures of gasses [mmHg] in lieu of parts per million [ppm]). When relevant to the present subject the exact values will be presented in habitually used units of measurement for the built environment.

The following data is currently available about the artificial atmosphere on the ISS and correspondingly for the CQ cabin. The composition of the atmosphere strives to be the same as that on Earth at sea level (same gas concentrations at the same partial pressures). Parameters of the artificial atmospheres to be monitored are the partial pressure of oxygen (ppO₂) and carbon dioxide (ppCO₂), temperature, relative humidity, air velocity and noise [4].

The partial pressure, ppO_2 , will be maintained between 155-380 mmHg (interval for which there is no quantifiable impact on human performance), the optimal range being between 139-178 mmHg. $ppCO_2$ has no lower limit on health, so the range is 0-5 mmHg (0-6500 ppm; for reference at sea level CO_2 concentration is 415 ppm). The temperature is to be maintained between 18-27 °C on the ISS corridor, with a relative humidity between 25-75%, the optimal range being 30-50%. In terms of air velocity, ISS requirements state that, based on empirical evidence, two-thirds of the internal atmosphere should have a velocity of between 4.6 - 36.6 m/min (0.076 – 0.61 m/s) considered to be sufficient for avoiding CO_2 accumulations or high temperature areas [4].

Data concerning the maximum time allowable in an area as a function of CO_2 partial pressure indicates that for the average 8 hours of sleep the CO_2 concentration must be below 10 mmHg (13000 ppm). Standards for the built environment [13] state that CO_2 levels inside working spaces should not surpass 10 times the concentration found in the fresh air outside (so for sea level parameters the limit would be 4150 ppm). A significant difference in scale becomes evident when comparing spacecraft recommendations to those of the built environment, the question is what causes this difference and how significant is it for the astronauts?

To answer this question, we turn to studies concerning the tolerance of astronauts and humans in general to heightened levels of CO₂ concentration. As previously mentioned, CO₂ as an intoxicant and a hazard to human health is a subject that is well known and always taken into account when designing spacecraft [2–4]. Initially the removal of CO₂ from the ISS atmosphere was to be handled by the Carbon Dioxide Removal Assembly (CDRA – part of the ECLSS), even installing two of them aboard the ISS [4]. Later reports [5,10] state that the energy consumption of the CDRA is not insignificant and that running the two CDRA's simultaneously is required to bring average CO₂ levels (varying for each ISS module) below 2 mmHg (2600 ppm). A single CDRA is designed to serve 6 crew members, being able to maintain a CO₂ level around 4 mmHg (4200 ppm). For comparison, 2 mmHg (2600 ppm) is still 6 times greater than the CO₂ concentration on Earth at sea level. It was reported [10] that running the two CDRA's

simultaneously is extremely resource intensive, and thus not a sustainable option. The report [10] concludes that operational levels of CO₂ below 3 mmHg (3800 ppm) are impractical from a hardware stand point, and that the CDRA should function only as necessary to ensure crew health and comfort.

Crew health, of course, goes hand in hand with the study of the CDRA and ECLSS. Several studies [3,10,11] have attempted to formulate recommendations for CO₂ operational limits based on crew performance and health reports. The performance evaluation was performed by the astronauts themselves since they learned to recognize symptoms of CO₂ intoxication as part of their training [4]. The reports [3,10,11] showed significant variability in the tolerance levels of the astronauts, to the extent that a clear upper limit of CO₂ concentration could not be established based on the data available. The main reason for this conclusion was the variable personal tolerance to CO₂ of each astronaut. Following these results, the practically unanimous recommendation was that CO₂ levels be kept as low as possible [3,10,11]. A note must be made about one of the reports [11] which concerned not only crew health and performance but also the human biology in microgravity. The report [11] stated that upon entering microgravity the human body starts to adapt to the environment, and that during the adaptation period (which varies for each individual) CO₂ intoxication symptoms are very common, but that they subsequently subside after acclimatization is complete (up to two weeks).

It becomes clear that the problem of CO_2 accumulation depends as much on the environment (ventilation and CO_2 removal facilities), as on the biology of the astronauts themselves. This prompted the investigation, in the following sub-sections of the presents thesis, of the human mechanics of breathing, CO_2 absorption and retention and the investigation of an efficient way to design a ventilation system which covers the weaknesses of the existing hardware without brute forcing them (i.e., increasing the flow rate by considerable amounts as a solution to the problem of insufficient ventilation).

Knowing an upper limit of CO₂ concentration is an important factor for crew health, however it is insufficient. When thinking about concentration limits it is a common assumption that the concentration is uniformly distributed in the studied enclosure. Returning to the problem of CO₂ pockets, it becomes clear that the average concentration levels monitored by the CDRA need to be supplemented with CO₂ data from poorly ventilated regions, which can reach concentration levels far above the module averages [10]. To this end, numerical simulations (CFD studies) were used as a tool to help in identifying regions susceptible to CO₂ accumulation. CFD studies offer the advantage of enabling the study of the environment in microgravity (impractical on Earth-based facilities) and offer indications as to where the astronauts might conduct experimental measurements, should they be required.

The primary step in considering the use of CFD models for a solution is to study their applicability to the problem in question. To this end we find several studies [14–20] which use virtual models of the ISS corridor to study the general ventilation.

Only one of the above studies [16] is directly validated with experimental measurements (of a confidential nature as previously mentioned), however the other studies using the same recommendations [17–20] are accepted just the same. This leads to the conclusion that CFD simulations running RANS models are suited and accepted for the study of the ISS general ventilation environment. Indeed, CFD models should be used due to the impossibility of reproducing the conditions of microgravity in our research facility. In addition to the general

ventilation study, our attention must be directed towards the process of CO₂ generation and accumulation.

A study of the ISS corridor [14] is closer to our problem of CO₂ accumulation in the CQ. The paper [14] dates from 2002 and investigates in CFD a case of fan failure in the old resting areas with a breathing astronaut (Figure 3, the alcove with the human model inside) when the astronaut is present inside and the ventilation system is switched off. The purpose of this study was to assess the risk of asphyxiation if the internal ventilation system of the cabin fails leaving only the general ventilation system of the ISS corridor running (Figure 3). A simplified model was used for the astronaut inside the cabin, with a 500 thousand cell mesh. The source of carbon dioxide inside the cabin is the astronaut's nose. The simulation was performed in steady-state for the initial case on the basis of which a transient simulation was subsequently performed with a time step of 0.2s.

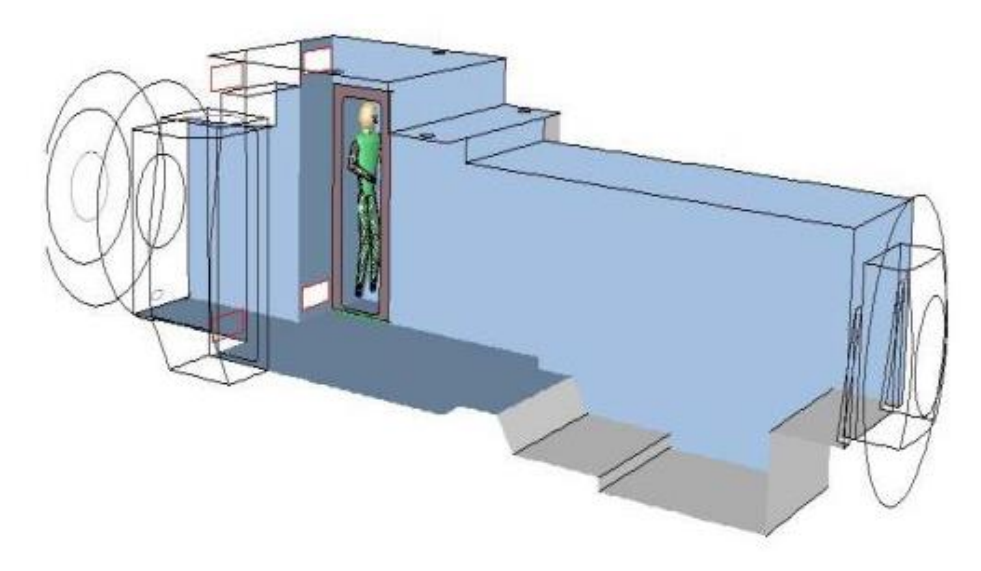


Figure 3 Old resting areas and ISS corridor [14].

The model in Figure 3 has several air supply inlets (the rectangles with red borders in Figure 3) situated near the old resting area, represented by the alcove with a human inside, supplying a flow rate of 85 m³/h for each resting area until a point in time at which the fans are turned off and the flow rate becomes null. From that point, with a time step of 0.2s the accumulation of CO₂ is studied inside the old resting area for a period of 10 minutes. CO₂ emissions were imposed according to NASA's estimated daily CO₂ emission rate [14,21] for sleeping crewmembers (0.32 m³/day), a respiration cycle of 12 breaths per minute, and the average duration of an expiration (3 seconds). The nostrils are represented by circles with a diameter of 0.635 cm each. The flow rate of the expiration is not given, but we know it is calculated from the average quantity of CO₂ generated by a crew member during sleep as indicated in NASA's human physiology manual for outer space exploration [21].

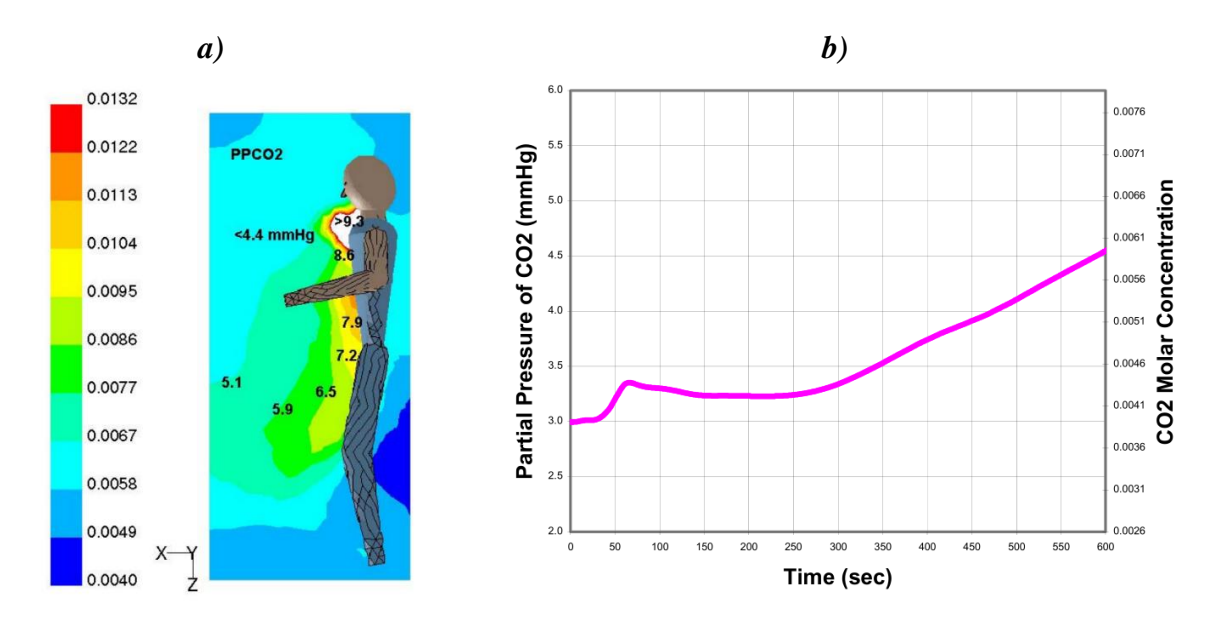


Figure 4 CO₂ molar concentration and partial pressure contours around the astronaut after 10 minutes (a) and CO₂ accumulation over time in the breathing zone (source: [14]).

Figure 4a shows the molar concentration (color map) and partial pressure contours of CO₂ (black values) after 10 minutes in study [14]. An accumulation of CO₂ is found in front of the neck and torso area, with the concentration decreasing further away from the body. The highest partial pressure values in front of the torso are over 9.3 mmHg. The authors plotted the variation of CO₂ molar concentration and partial pressure at a point 20 cm in front of the astronaut model's neck in the positive direction of the X-axis (see Figure 4a for axis orientation) over the course of the 10 minutes of simulation (Figure 4b). The oscillations at the start of the graph presented in Figure 4b are not explained in paper [14] but can probably be attributed to the numerical model's instability during the first iterations. The point where the data was extracted for Figure 4b is questionable as it is not situated in the direction of the exhaled breath. On the other hand the method of CO₂ generation in study [14] gives is based on an equivalent generation of CO₂ by a human defined as a constant flow rate, not taking into account the dynamics of breathing.

Looking at Figure 4a, it would appear that after 10 minutes the local accumulation of CO₂ in front of the neck and chest area risks of surpassing the 10 mmHg (13000 ppm) partial pressure limit. It is clear that such an accumulation rate is not sustainable during 8 hours of sleep, and would endanger the astronaut due to local pockets of carbon dioxide forming. We must recall that this example serves to illustrate the gravity of the problem of CO₂ accumulation, and not an ordinary occurrence, as the no-ventilation scenario presented [14] is, in itself, an emergency in regards to the safety of the astronauts.

This model highlights two important factors in the study of CO₂ pocket formation: (1) the orientation of the CO₂ source (in this case the nose) plays a key role, as expiring towards the chest makes CO₂ accumulate in that region; and (2) the CO₂ generation model used is important. In the above case [14] a constant CO₂ flow rate was imposed, meant to be the equivalent of the overall CO₂ generated by the astronaut over a period of time. Although this approach is correct in regards to mass balance it also highly favors the formation of CO₂ pockets through the constant low flow rate of the exhaled air.

A dynamic breathing model, representing both the inhalation and exhalation cycles would produce higher peak velocities potentially distributing the CO₂ in a different manner. Another issue that needs to be addressed is the dependance of CO₂ pockets upon the head position. A CO₂ pocket forming is not dangerous for an astronaut unless it forms in the region from which he draws air, termed as the breathing zone [2,4,10,11]. The definition of the breathing zone is vague in these studies [2,4,10,11], but an idea forms that accurately identifying this zone enables us to tailor a ventilation solution that specifically targets it, potentially eliminating the need for augmenting the flow rate within the CQ.

The subject of Stage 1 in the present thesis is the study of the CO₂ generation and accumulation as well as the accurate identification of the breathing zone. An in-depth study about how the breath can be accurately represented and how the breathing zone is determined will be treated in Section 1 of the Introduction. Presently, the following step in the study of the ISS CQ, is to identify what improvements can be made to the existing ventilation solution of the CQ.

The problem of air circulation in the enclosed cabin space of the CQ can be compared with a ventilation study in a room, but is in fact complicated by the lack of the ability to accurately reproduce the operating conditions (especially the extremely weak gravitational field) in an experimental setting. Velocity values at different points of the CQ ventilation system were evaluated aboard the ISS by the astronauts [9] using a TSI Velocicalc Ventilation meter [22] (the exact model was unspecified).

The CQ velocity measurements on the ISS [9] were taken at the exhaust duct outlet (Figure 1) and at the diffuser grille (Figure 2b). Results show velocity values between 0.5 and 4.5 m/s for the exhaust outlet for the medium fan setting (as previously described in [7,8]) and between 0.15 and 0.3 m/s when measured in front of the diffuser (at an unspecified distance) centered on each of the flow channels (Figure 2a). These values varied according to the measurement position and according to which CQ they were measured in (measurements were made in two out of the four CQ installed). The report [9] mentioned that this variability exceeded expectations and attributed it to turbulence, complex flow fields and insufficient instrument capability.

The same report [9] highlights instances of significant dust accumulation in the ventilation ducts, sometimes leading to a decrease in flow rate to the point that the CQ fan alarms are set off by the flow detectors in the ducts because of insufficient flow [8,9]. Regular cleaning of the ducts for dust removal was recommended, as dust was seen as a significant factor affecting the flow rates and even presenting risks of damaging the sensors in the ducts [9]. It is unknown in what state of cleanliness the ducts were during the measurements [9]. Despite the influence of the dust, and the instrumental apparatus used, the report [9] formulated the general conclusion that the fans provided acceptable flow rates in general, but that there is a significant variability between the different CQ cabins.

Another attempt to characterize the flow rate inside the CQ was made in study [8], where the velocity distribution across the inlet diffuser (Figure 5) was measured. The measuring equipment was not specified [8], but seeing as the measurements were made on-board the ISS, it can be assumed that a ventilation meter similar to the one described in [9] was used. Similarly the measurement protocol was not described [8] so the distance at which the measurements were performed is not precisely known, only the number of points (138). The location of the five flow channels delimited by the flow guide vanes (Figure 2b) are marked in Figure 5 with letters from A to E. The velocity distribution across the inlet diffuser is not uniform (Figure 5) despite the

addition of the guide vanes, whose original purpose was to evenly distribute the flow. Higher velocity values are found near the guiding vanes themselves, as evidenced by the vertical regions of higher velocities (seen between the letters in Figure 5). The highest velocity regions are found towards the top of the diffuser inlet between guiding vanes A and B, and B and C respectively.

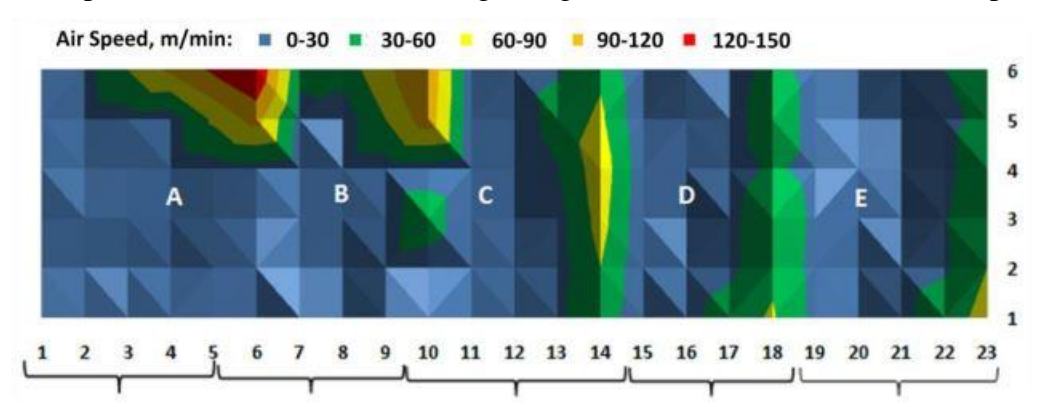


Figure 5 Inlet diffuser velocity distribution with the five channels delimited by the flow guide vanes (Figure 2b) marked from A to E (source: [8])

The uneven air distribution in Figure 5 presents itself as the first aspect that can be improved and consequently which warrants investigation. A more uniform velocity distribution would reduce the likelihood of poorly ventilated regions appearing. The velocity distribution is heavily dependent on the ventilation circuit behind the diffuser and improving the distribution likely implies changing the ventilation circuit itself.

Looking at Figure 5 it appears that the resolution of the inlet diffuser velocity distribution is insufficient as evidenced by the sharp edges visible at the center of each diffuser orifice, so any attempt to validate CFD models using these data would be qualitative at best.

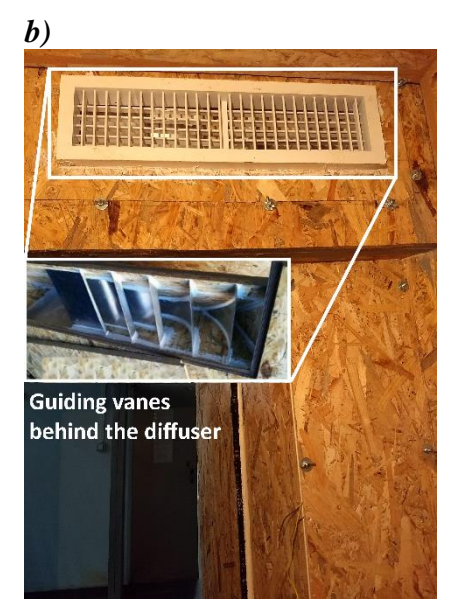
Diffuser velocity distributions are habitually used in building ventilation to describe inlet conditions especially in CFD models (which, as previously established, are a requirement in this case). Obtaining a higher resolution velocity distribution would require the construction of a full-scale experimental model in our research facilities featuring identical ventilation circuits and fans. The measurements would require high precision equipment and techniques (such as laser doppler anemometry (LDA) or particle image velocimetry (PIV)) capable of capturing a high-resolution velocity distribution.

A full-scale experimental model of the CQ is the first challenge of the present thesis. Such a model could be used to study the existing ventilation solution on Earth, with the experimental results being used in CFD simulations of microgravity conditions. A full-scale model would aid in the study of CO₂ generation and accumulation as well as for acoustic measurements.

To design the full-scale CQ model, the dimensions of the CQ were deduced from the available documents [7–9]. No detailed plans of the CQ exist, so it must be noted that although the authors reconstructed it as best as they could from the information available, some small inaccuracies may exist. The walls of the full-scale CQ model were built out of plywood (Figure 6). The view from the exterior is seen in Figure 6a, the walls were painted black and the intakes and outflow grilles were painted white. At the CQ's interior the diffuser inlet grille can be seen near the top of the CQ in Figure 6b. Below and to the right of the diffuser grille are the fan ducts

and the axial fan itself hidden (as seen in Figure 6c).





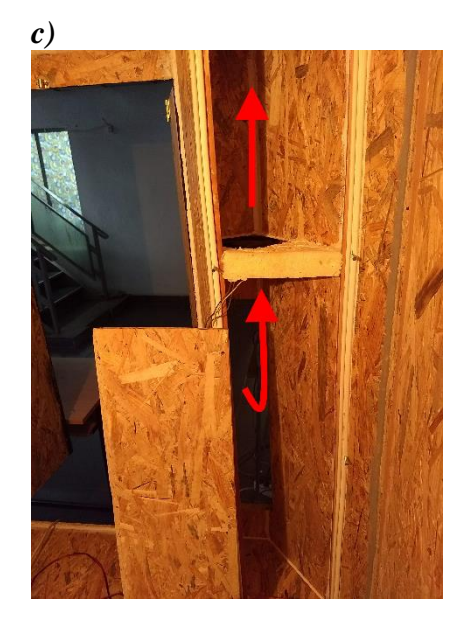


Figure 6 Full-scale CQ model during its construction: exterior view (a), interior view featuring the diffuser grille (b) and interior view of the intake's axial fan (c).

The axial fans used in the full-scale are identical to the ones in the ISS CQ uses (EBM Pabst 4184 NXH compact axial fans. One fan was installed in the intake circuit the other in the outflow circuit. The fans are powered via a 24V direct current connection. Figure 6 was taken just after the model's construction, but subsequently the interior CQ walls as well as the ducting system was lined with the same soundproofing materials used for the ISS CQ [8]: a three-layer quilted-structure made from Kevlar® wool pad, white Gore-Tex® and Nomex®. The lining of the walls helps mitigate the transmission of acoustic waves through the walls and ducts of the CQ.

The complex intake air circuit previously presented in Figure 2 was reproduced as best as possible. The circuit in the full-scale CQ model features two elbows (90° and 180°) just as the ISS CQ does. The guiding vanes behind the diffuser grille (Figure 2b) are also present. The outflow circuit situated in the lower part of the CQ is shorter without any notable characteristics. We recall that the intricate circuit helps dissipate the background noise from the ISS corridor as well as the ventilation circuit fans [7,8].

An issue becomes readily apparent however, namely that the size of the model, renders it impractical for using high resolution velocity measurement techniques such as PIV or LDA without significantly altering its design and adversely affecting secondary model characteristics such as acoustic performance. At the same time the CQ (Figure 1) is too small to perform high resolution measurements at its interior, constraining the measurement of velocity distributions to portable anemometers, risking the same issues as the measurements aboard the ISS. A potential solution to this conundrum presents itself in the form of the fans used in the ventilation circuit and their operating curves as described below and detailed in sub-sections 3 and 4 of this chapter.

During the design process of the CQ [7,8], fan choice was based on several factors such as acoustic performance, pressure head capabilities, size, robustness (low failure rates) and their capability to reduce heat buildup. The procedure for testing the fans was mounting them in an

experimental stand (Figure 7a) in order to measure their power/pressure and flow performance. This evaluation of performance was based on the fan's performance curve, which is regularly plotted against the system resistance curve, giving the operating point of the installation (Figure 7b). At the operating point, the flow rate through the system can be read in a pressure head – flow rate plot.

Determining a fan performance curve requires installing the fan in an experimental stand in which the head losses can be varied, while measuring the flow rate and the pressure head at each point with a flow meter and a manometer (as seen in Figure 7a). Additionally, fan power draw was measured during the CQ design phase. Two fans were required for each CQ cabin, for backup in case one of the fans were to fail. The fan performance curve can be used to evaluate the configuration of two or more identical fans installed in series or in parallel as was done in Figure 7b. The acoustic performance of the fans was not tested prior to fan selection from the information that is available [8], but were instead performed at a later stage in the CQ cabin design process.

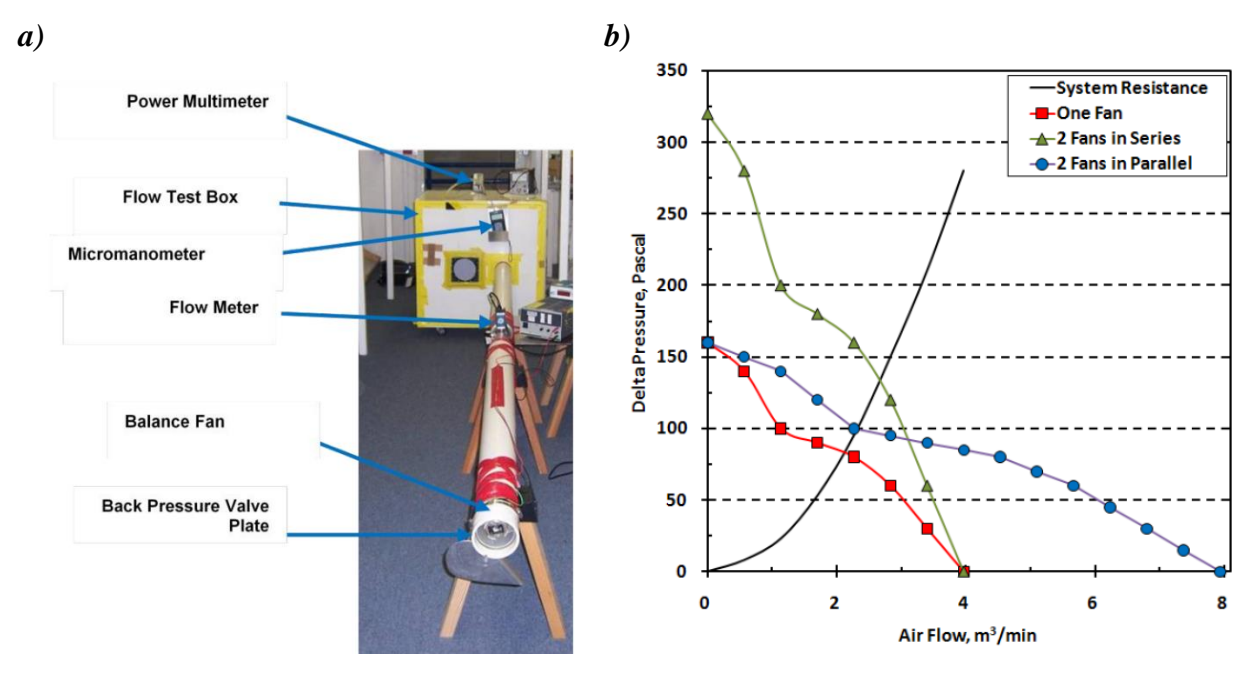


Figure 7 The measurement stand used in the CQ design process (a) and the measured fan performance curve versus the system resistance for different fan configurations (b) (source: [8])

Out of a selection of five fans that were measured [8], the one chosen for use in the CQ cabins was EBM-Papst 4184 NXH as a compromise between its size, power efficiency, pressure and acoustic performance. The two fans were mounted in series, because of the abrupt slope of the system curve caused by the head losses along the intricate ventilation circuit (Figure 2).

When setting up the fan controls for the ventilation system, the heat build-up was also taken into account and the maximum flow rate was limited to 156 m³/h as going beyond this limit led to diminishing returns in reducing heat build-up and risked a significant increase in generated noise. Allowing a continuous control of the fan rotation speed was considered [8], but was ultimately rejected as an option due to the complex electrical components required for the fans that could cause reliability issues. In order to allow the astronauts some degree of control over the flow rate

inside the CQ cabin, three pre-defined fan rotation settings were created for three different flow rates: 108 m³/h (low fan setting), 138 m³/h (medium fan setting) and 156 m³/h (high fan setting).

The experimental setup for measuring fan operating curves is inexpensive to recreate and can be used in the eventuality that the improvement of the CQ ventilation system implies changing the fan. If the fan operating curves are measured, they can be imposed in CFD models as boundary conditions along with the fan rotation speed. This generates a flow through the numerical ventilation circuit which eventually stabilizes at what is called the duty point (the intersection between the fan operating curve and the system resistance curve). The duty point gives the flow through the circuit. Turbomachine affinity laws (applicable to both fans and pumps) can then be used to determine the fan rotation speed required for the fan to provide a desired duty point in the experimental or numerical setup.

For the study of the axial fan used in the CQ and for an eventual replacement fan the procedure would be the following: (1) measure the fan's operating curve at nominal parameters in an experimental setup; (2) use the operating curve as a boundary condition in a numerical model which accurately reproduces the CQ and its ventilation circuit; (3) alter the resulting flow rate, if necessary, by using the affinity laws to determine the required rotation speed; (4) validate the numerical results with experimental measurements to confirm that the numerical model works properly. After these steps are successfully completed, we can then use the numerical results to further our study of the CQ's ventilation system and its impact on CO₂ accumulation.

One important factor remains to be addressed: what experimental measurements will be used to validate the numerical results. The operating curves themselves are a kind of experimentally measured boundary condition, but the resulting flow field inside the CQ is what interests us. As previously stated, high resolution velocity fields at the diffuser cannot be obtained inside a full-scale model of the CQ due to its small interior volume. And while a comparison can be made between numerical results and the measurements in the ISS CQ (Figure 5), because of the latter's low resolution it would be a qualitative comparison at best.

In building ventilation studies, the flow fields inside a room often need to be determined, but the volume is too large to enable their direct measurement by highly accurate techniques (PIV, LDA). For this reason, we often find the use of reduced-scale models [23–25] in conjunction with PIV techniques for the study of flow fields inside buildings. Such PIV-measured flow fields, when scaled up, represent very reliable sources of validation for numerical results [26]. A similar approach can be used in the present case, by designing a reduced-scale model of the CQ, and using PIV techniques to measure the flow fields inside it. These experimental results can then be used to validate the numerical models using the fan operating curves as boundary conditions. If the numerical flow fields match PIV flow fields, then the fan models were able to accurately simulate the flow through the CQ.

The subject of Stage 2 in the present thesis is the evaluation of the existing flow fields in the CQ. The flow fields will be evaluated based on numerical results obtained by using the experimentally measured axial fan operating curves as boundary conditions in a numerical model featuring the full-scale CQ and its ventilation circuit. The numerical results will be validated with experimental PIV measurements in a reduced-scale CQ model made of transparent acrylic. After the validation the velocity flow fields obtained in this Stage will be compared to the CO_2 accumulation results from Stage 1, in order to identify regions inside the CQ in which the ventilation needs to be improved.

Recalling the ventilation circuit presented in Figure 2, the first aspect that can be improved is its complexity. The current ventilation circuit features numerous bends in its attempt to provide a uniform flow of air at the diffuser grille. This attempt is moreover not completely successful as can be seen in Figure 5, where the highest velocities are clearly found around the guiding vanes behind the diffuser grille.

Changing the diffuser circuit could be an option, but one must assume that an optimization study was done during the conception of the CQ cabins. It is a safe assumption that the current CQ ventilation configuration is close to optimal for its parameters (type of fan used, required flow rates and acoustic levels). An assumption is made at this point by the author, that an axial fan was chosen because of the requirement that the fan be powered by direct current (DC) as it is the only means of power supply on the ISS, and axial fans are often powered this way (e.g., cooling fans for PCs).

Replacing the axial fan (AF) with a cross-flow fan (CFF) could potentially improve the ventilation circuit. CFF solutions are used in indoor air conditioning units for their capacity to evenly distribute the flow of air over a larger surface as well as due to their good acoustic parameters making them ideal for indoor applications. In the context of the CQ the CFFs could fit into the upper and lower plenums of the rack frame (Figure 8), eliminating the need for the vertical ventilation ducts of the AF solution (Figure 8a₂). In addition, there would no longer be need for any guiding vanes behind the diffuser grille which could lead to a better air distribution across the diffuser. Finally, with the removal of the ducting and guiding vanes the overall weight of the CQ would be removed, reducing the costs of sending it into space.

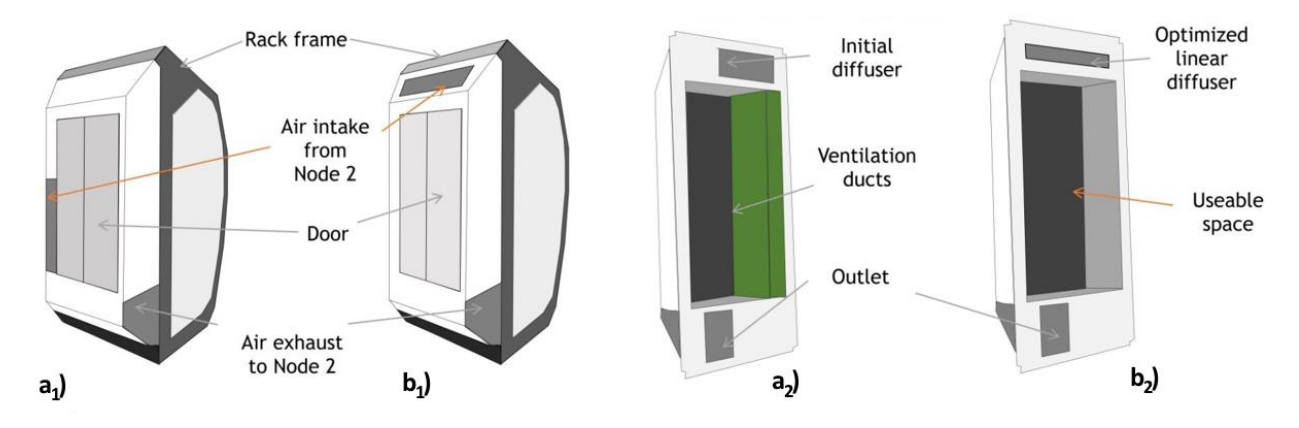


Figure 8 Proposed improvement of the CQ ventilation circuit by replacing the AF circuit (a) with a CFF circuit (b) – external (1) and internal (2) views.

The replacement of the AF ventilation solution with CFFs represents the first step of improving the CQ ventilation system. The evaluation of the CFFs will be the subject of Stage 3. In a similar manner to the AF used in the CQ, CFFs of equivalent parameters will be selected, their operating curves measured experimentally and then imposed as boundary conditions in CFD models featuring a different ventilation circuit more suited to the CFFs. Velocity flow fields inside the CQ will be evaluated for the CFFs and compared with the AF velocity fields previously validated by PIV results. In addition, in the full-scale model of the CQ the CFF acoustic performance will be evaluated and compared to that of the AF both in our full-scale experimental models as well as with acoustic data from the ISS CQs. The final stage (4th) of this study covers

the case in which the CFF solution does not remove CO₂ from the occupant's breathing zone fast enough, a final contingency is considered: the implementation of a personalized ventilation solution supplying a stream of fresh air directly to the breathing zone.

Personalized ventilation (PV) solutions have been extensively studied in problems related to indoor air quality [27–29]. The basic idea is to supply fresh air directly to the occupant, penetrating through the convective boundary layer of the human body (absent in microgravity in our particular case). There have been several proposed methods for accomplishing this, from a diffuser supplying the air directly to the occupant's face [27,30,31], to devices integrated in office furniture [29,32] or even in chairs [33,34].

PV solutions typically supply a lower flowrate than building environment standards [35,36] would suggest is required by each occupant. The low flow rate is acceptable because it is used in its entirety to ventilate the only region of importance for inhaled air quality – the breathing zone. The PV flow rate required is not set in stone as it depends on the distance between the PV diffuser and the occupant as well as on the orifice shape and size of the diffuser [37–39]. The general consensus is that velocity values above 0.3 m/s need to be obtained from the PV diffuser in order for the ventilation jet to penetrate the convective boundary layer of the human body [40–42].

For the present case regarding the CQ the PV system has fewer obstacles than on Earth studies would suggest. First of all, in microgravity, the human convective boundary layer is inexistent. Thus, the recommended minimum velocities for penetrating the CBL (0.3 m/s) are not applicable, opening up the possibility that the supplied velocities can be even lower. Secondly, there is little option in regards to the type of PV diffuser to be implemented, as the occupants of the CQ are not situated in seats nor do they have desks or other furniture in which PV systems could be implemented. The only option left is to supply the fresh air via a PV diffuser oriented towards the breathing zone.

Three design questions remain for the CQ PV system: (1) where shall the PV be mounted – ideally it would be supplied passively from the CQ ventilation circuit; (2) at what distance from the occupant is the PV diffuser to be installed and finally (3) what shape will the diffuser have.

The study of the implementation of a PV system in the CQ will be the subject of Stage 4 of the present thesis. In this stage, PV diffuser velocities and effects on human comfort will be studied. An in-depth description shall be provided of the effects of different PV diffuser orifices and their influence on the air flow and comfort sensation. Finally, different PV diffuser positions will be studied in the attempt to optimize the diffuser's placement in the CQ. CO₂ accumulation in the CQ will be studied as part of Stage 4 for comparison purposes with the CQ with its regular (AF) ventilation system as well as with the proposal for the CFF ventilation system, in order to quantify the impact of the PV solution.

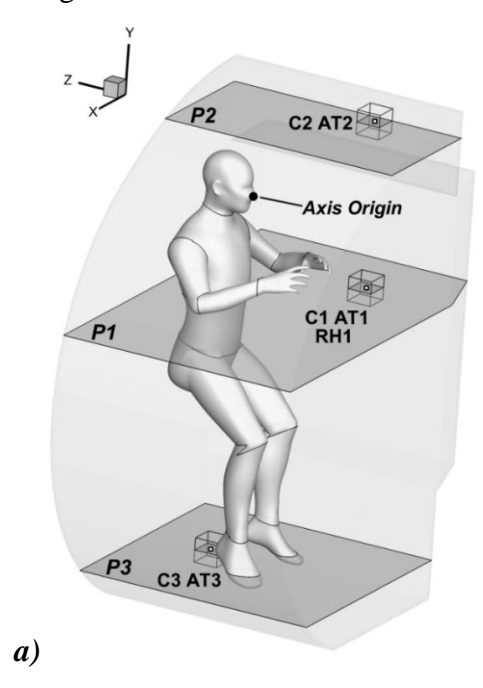
The following sections of the present thesis Chapter will go into an in-depth study of the literature available for Stages 1 through 4 of the experimental study, and discuss the design requirements and potential impact of each solution for the CQ.

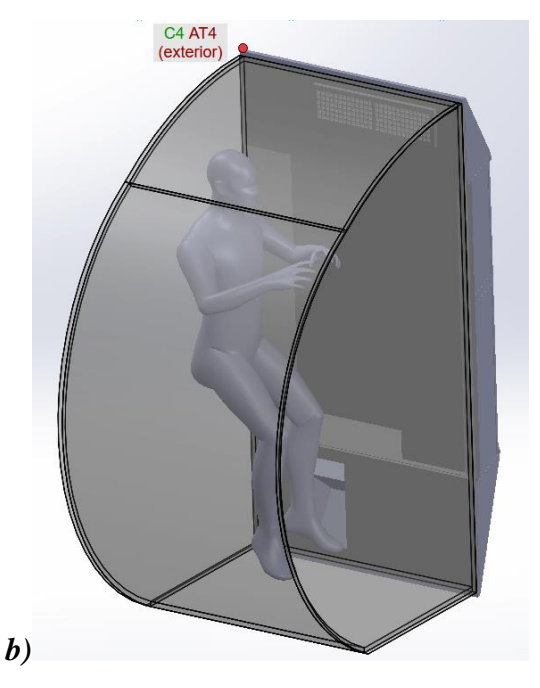
I. Modeling of a realistic respiratory cycle and analysis of carbon dioxide accumulation in the breathing zone

The first paper studies CO₂ accumulation in the CQ. The study is based on experimental measurements taking place in the full-scale CQ model with different human subject. CO₂ was recorded at three different locations with the CQ model closed and the ventilation system turned off. 13 test subjects took part in the experiment. Aged between 22 and 50, with heights ranging from 1.65 to 1.89 m and weights in the 65-110 kg interval. Of the 13 subjects, there were 10 males and 3 females.

The CO₂ was measured for 15 minutes for each subject. Temperature and relative humidity were also measured as part of these tests. Subjects were seated on a high chair with their feet on a foot-rest above the ground mimicking the position likely assumed by the CQ occupants during sleep. Each subject was told to record their number of breaths over a minute at least thrice during the test. Otherwise, instructions were to behave as normal while at rest.

CO₂ concentrations were logged once every two seconds (0.5 Hz) and temperature and relative humidity were recorded once every 15 seconds (0.066 Hz). In total there were four CO₂ sensors – three inside the CQ (C1-C3) one outside as a reference (C4); eight temperature sensors (thermocouples) – seven inside the CQ three measuring air temperature (AT1-AT3) and four measuring wall temperature (WT1-WT4) with a fourth air temperature sensor outside (AT4); and finally, one relative humidity sensor inside the CQ (RH1). The positions of the sensors can be seen in Figure 9.





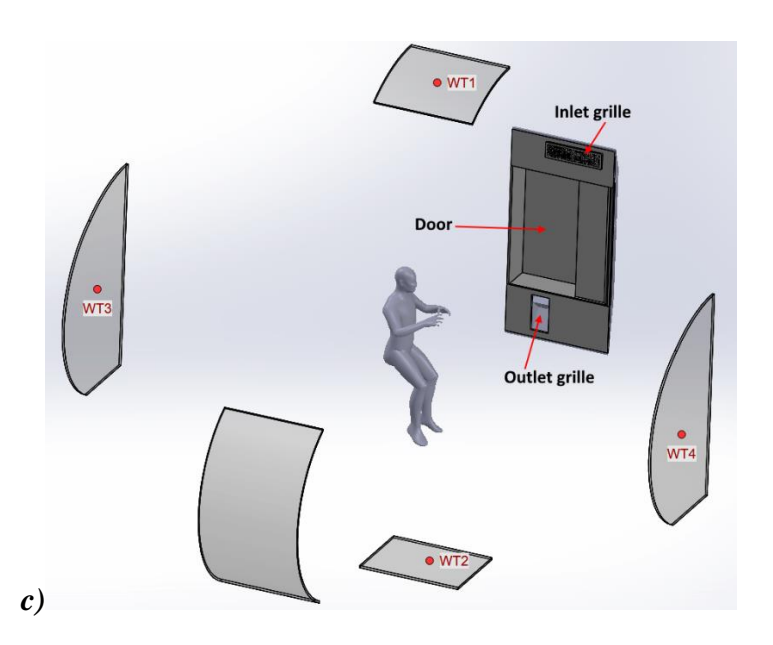
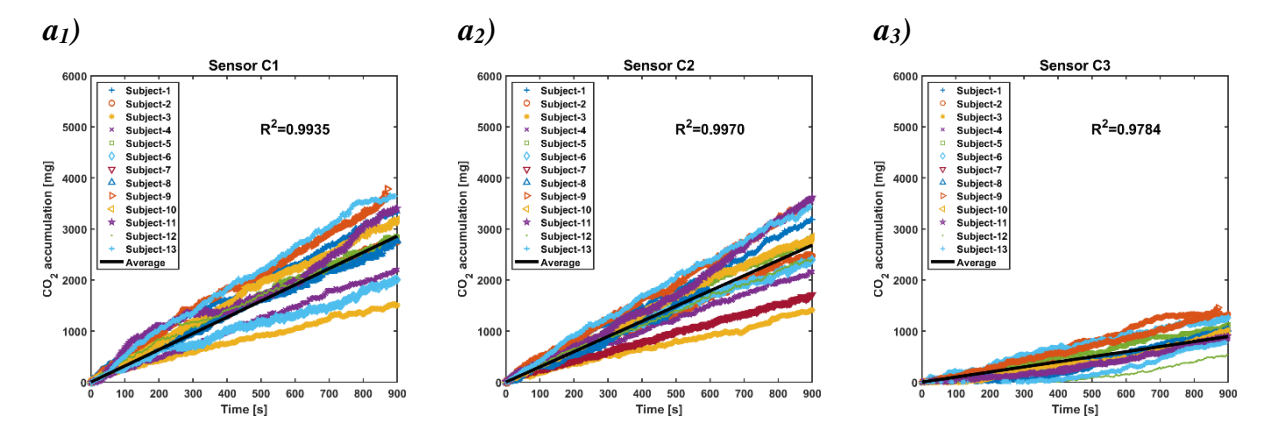


Figure 9 Experimental measurement for measuring CO₂ accumulation inside the CQ featuring the (a) interior air sensors, (b) the exterior air sensors and (c) the wall temperature sensors.

Because of the small interior volume of the CQ (<2.5 m³), and because there is no ventilation during the measurements, CO₂ levels registered by sensors C1-C3 could reasonably approximate the average concentration over a volume of air assigned to each sensor. Care was taken to place the CO₂ sensors away from the breath so that their measured values are the result of the CO₂'s mixing and diffusion inside the CQ. Experimental results (Figure 10) show significant increases of CO₂ inside the CQ while exterior levels remain constant. Air and wall temperatures averaged around 27°C at the start of the experiments and increased by about 1°C after 15 minutes, on average. Temperature sensor WT3 was excluded from the results as it presented significant variations due to its proximity to the test subject's back. Instructions were given to avoid resting against the wall; however, it is unclear to what extent they were able to follow this requirement during the 15 minutes of testing. Initial relative humidity values averaged around 65% and rose on average around 5%.



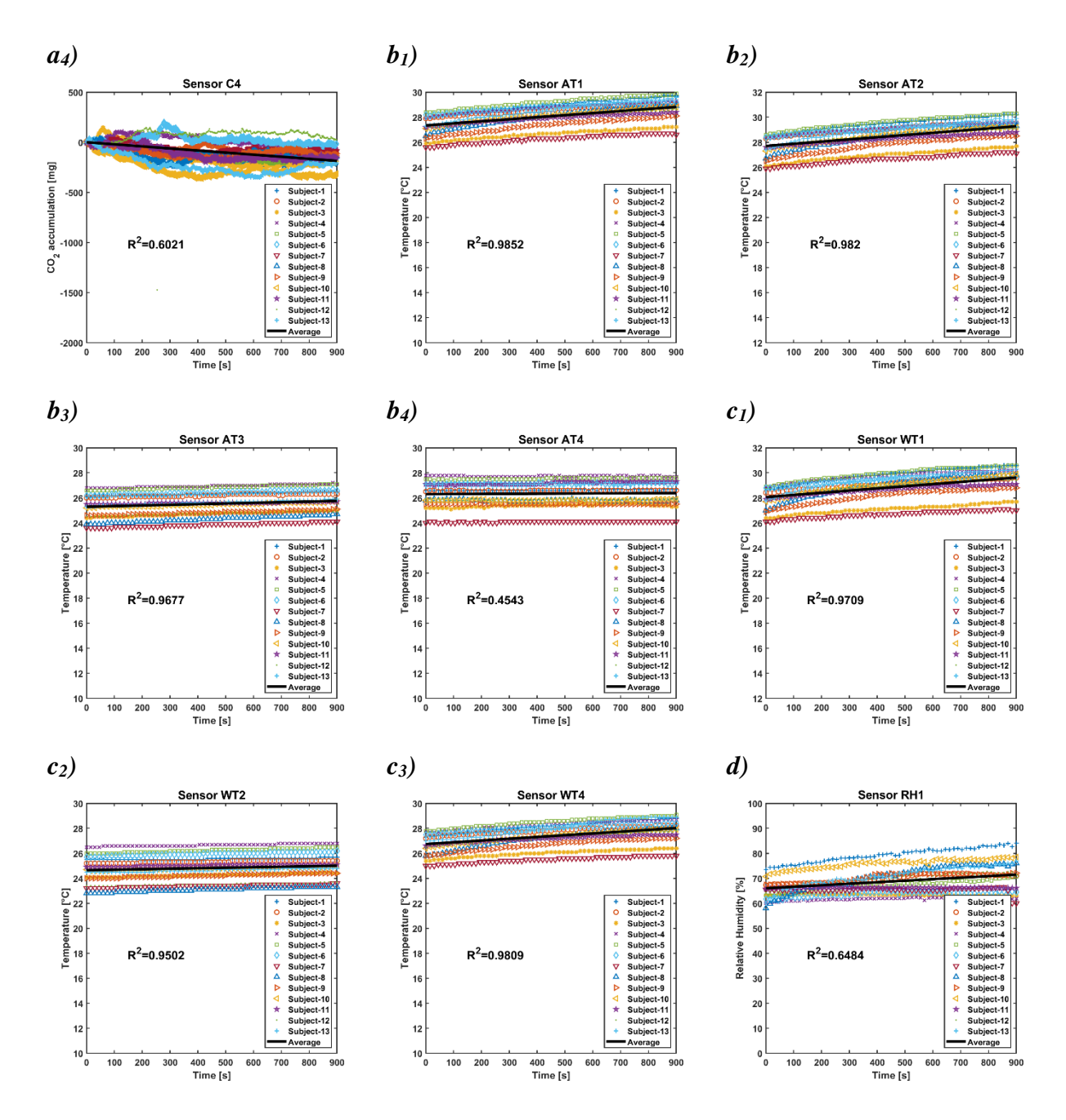


Figure 10 Recorded experimental results recorded of the CO₂ accumulation (a_1 - a_4), the air temperature (b_1 - b_4), the wall temperature (c_1 - c_3) and the relative humidity (d).

The experimental measurements formed the basis for numerical models of the CQ with a virtual human inside. The CO_2 accumulation results were used to calibrate a realistic breathing function imposed in the numerical model as a boundary condition. A numerical grid of 6 million tetrahedral elements was built with an average wall y^+ of around 1. Five layers were created to thicken the mesh near the walls.

The main components of air $-N_2$, O_2 , CO_2 and H_2O (vapors) were part of the species transport. Concentrations of O_2 and CO_2 in the ambient air of the numerical model were equal to

those at sea level: 21% and 0.04% respectively. H₂O vapor concentration was set so that the ambient relative humidity was around 65% at the start of the simulation. N₂ filled the remaining percentages so that the sum of all components equaled unity. Ambient air temperature in the model was set to 27°C, mimicking the average experimental conditions.

The air exhaled by the occupant was considered to have the concentrations specified in medical literature, namely 15% O₂, 4% CO₂ and sufficient H₂O vapor so that the exhaled air reaches 100% relative humidity. The exhaled air temperature was 36°C. Operating under the practical assumption that the above parameters are constant in the inhaled air, and that the human inhales air at sea level parameters, a CO₂ generation rate was determined. This generation rate was used as the basis of a sine-function representing a realistic breathing function along with the average breathing frequency of 14.7 breaths/min which resulted from the experimental measurements. The breathing function is described by the following equation:

$$u = 5.49 \cdot \sin(2\pi \cdot 0.245 \cdot t)$$

Despite the simplified assumptions, in the numerical simulation the occupant will inhale air at ambient values. The occupant will also be heated, mimicking the varying temperature of different body parts in order to generate a convective boundary layer. A transient simulation was run for 60 seconds in order to compare the CO₂ accumulation over this time period with the experimentally measured accumulation. The comparisons of CO₂ accumulation are shown in Figure 11.

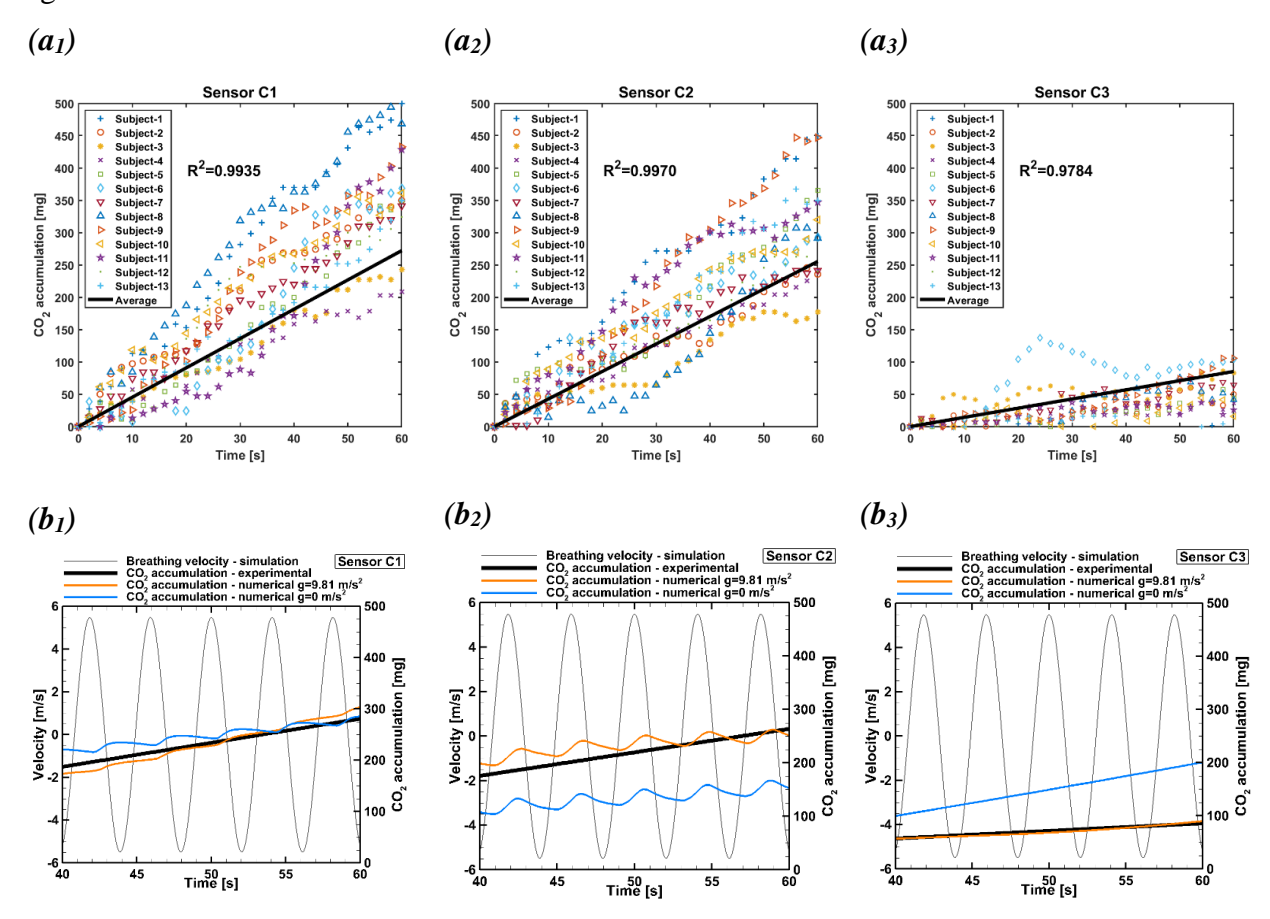


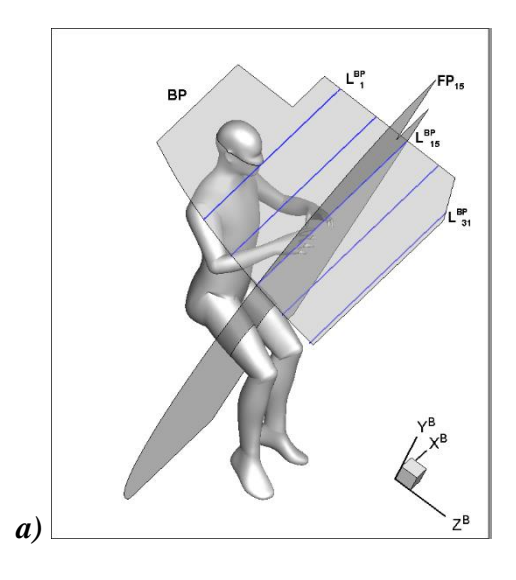
Figure 11 CO_2 accumulation in the experimental model over 60 s (a_1 - a_3); numerical and experimental CO_2 accumulation data at sensors C1-C3 (b_1 - b_3) (d) – the breath's velocity was superposed to study its effect on CO_2 accumulation.

Numerical CO_2 results were found to be in agreement with the experimental results. Overall CO_2 quantities in the CQ rose by about 600 ppm in both numerical and experimental cases. Average air and wall temperatures in the numerical model show average increases of around 0.1 °C after 60s. This is in agreement with the experimental measurements and since the accuracy of the experimental thermocouples is ± 0.1 °C between 0°C and 60°C, the temperature can be considered constant over the 60s of simulation. Relative humidity values showed an increase of 0.7% in the numerical model. They too were considered constant as the result in way below the accuracy of the relative humidity measurement equipment ($\pm 2\%$).

The good agreement of the CO₂, temperature and relative humidity comparisons is taken for validation of the numerical model employed. An additional numerical simulation was run on the validated model, without gravitational acceleration and the CO₂ accumulation between the two numerical cases was investigated. Results confirmed the suspicion that CO₂ tends to accumulate in front of the occupant's face.

An analysis of the dynamics of the breathing flow was undertaken in order to determine a rigorous method for defining the BZ. Due to the periodic nature of the breath (represented as a sine-wave) the BZ can be evaluated based on the breath's influence over the surrounding air. Fast Fourier Transforms (FFTs) can be used to identify patterns in the variation of a signal – such as the air velocity in the present case. If the FFTs applied to a region in front of the mouth show a pattern of air velocity variation at the same frequency as that of the breath (14.7 breaths/min) we can consider that the region in question is influenced by the human breath.

The study was be undertaken in two relevant planes for the occupant's breath: the plane perpendicular to the nostrils dubbed the breathing plane (BP) and the median plane of the head (MP). In each plane several lines were extracted (Figure 12) and FFTs taken in each point along these lines.



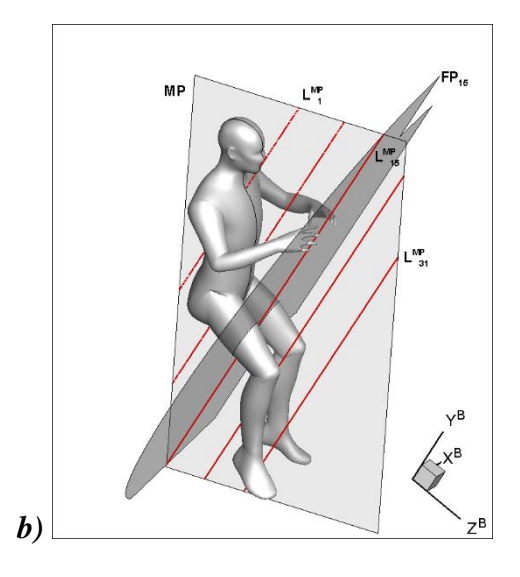


Figure 12 Lines for the FFT study in the breathing plane (a) and in the median plane (b)

FFT results along the lines in the BP and MP will aid in delimiting the zone influenced by the breath both vertically and horizontally. Three theoretical zones of influence were determined by a theoretical analysis of the breathing function's FFT results. The theoretical upper limit (l_1) represents perfect synchronization with the breathing function and is likely impossible to achieve in the study of the simulation results. The intermediate limit (l_2) represents perfect synchronization with a half-breathing cycle (either only the positive or only the negative halves of the sine wave). Finally, the lower limit (l_3) represents an average of multiple white noise signals.

FFT values between l_1 and l_2 indicate a strong influence of the full breathing cycle. Values between l_2 and l_3 suggest a weaker influence of the breathing cycle or if further away from the nose, likely the influence of the exhalation by itself. Finally values below l_3 are likened to white noise and will be used to delimit the BZ. Plots of the FFT values along several lines in the BP and MP planes are shown in Figure 13.

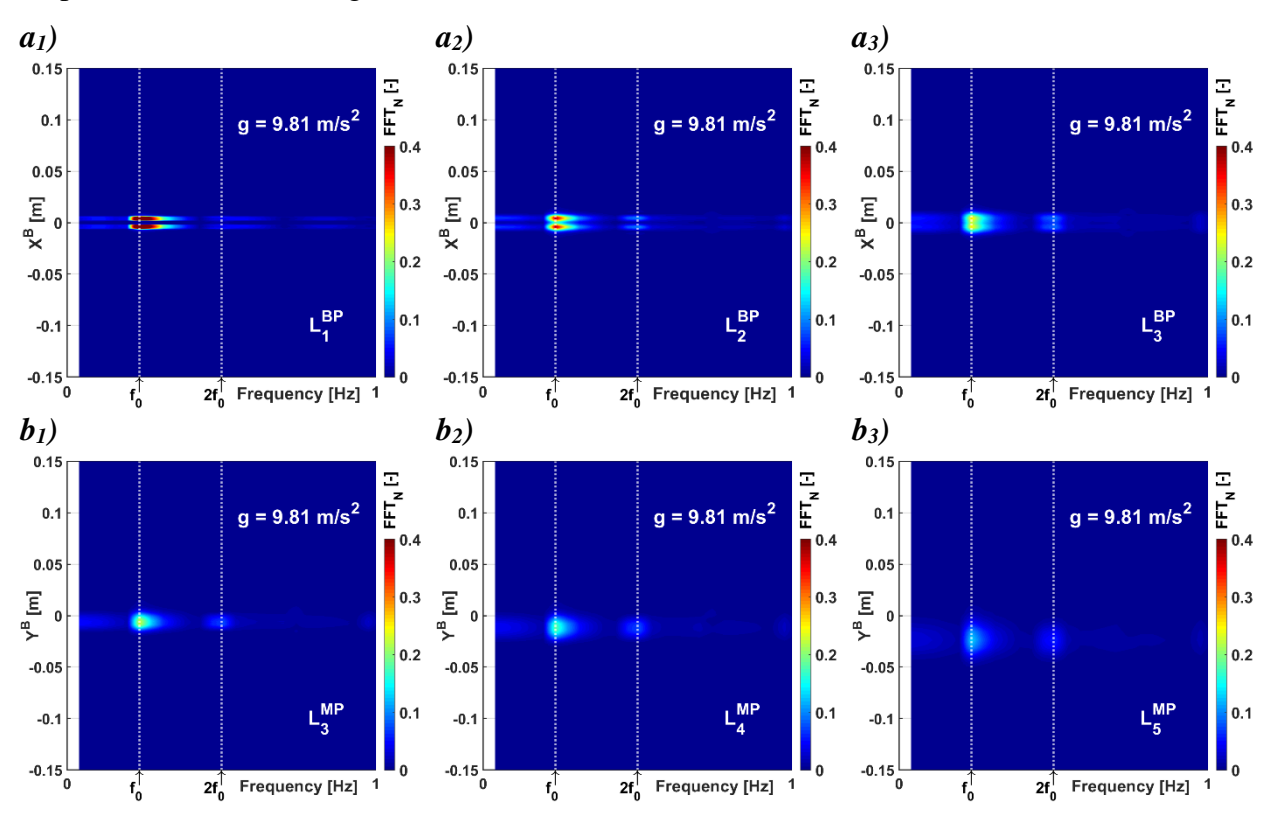


Figure 13 FFT investigation of air velocity in each point along the BP (a_1-a_3) and MP (b_1-b_3) lines.

The geometric extents of the BZ for the present case were determined based on the FFT method and the result was a region with a diamond-like shape in front of the nose. The BZ was 10 cm in length, and between 2 and 2.5 cm in width. It is worth mentioning that the FFT study for both numerical cases (with and without gravity) and no perceptible difference in the BZ was identified. This suggests that the FFT method is robust, being seemingly unperturbed by the presence of the convective boundary layer of the occupant in the case with gravity.

The BZ thus determined is shown in Figure 14a with highlights of the regions influenced by the full breathing cycle as well as those influenced by the half breathing cycle. Additionally,

the difference in CO₂ concentration between the numerical case without gravity and the case with gravity is presented in Figure 14b. Here, positive values indicate a CO₂ surplus without gravity, and the results show that in almost all of the BZ, there is a surplus of CO₂ by comparison to similar situations on Earth.

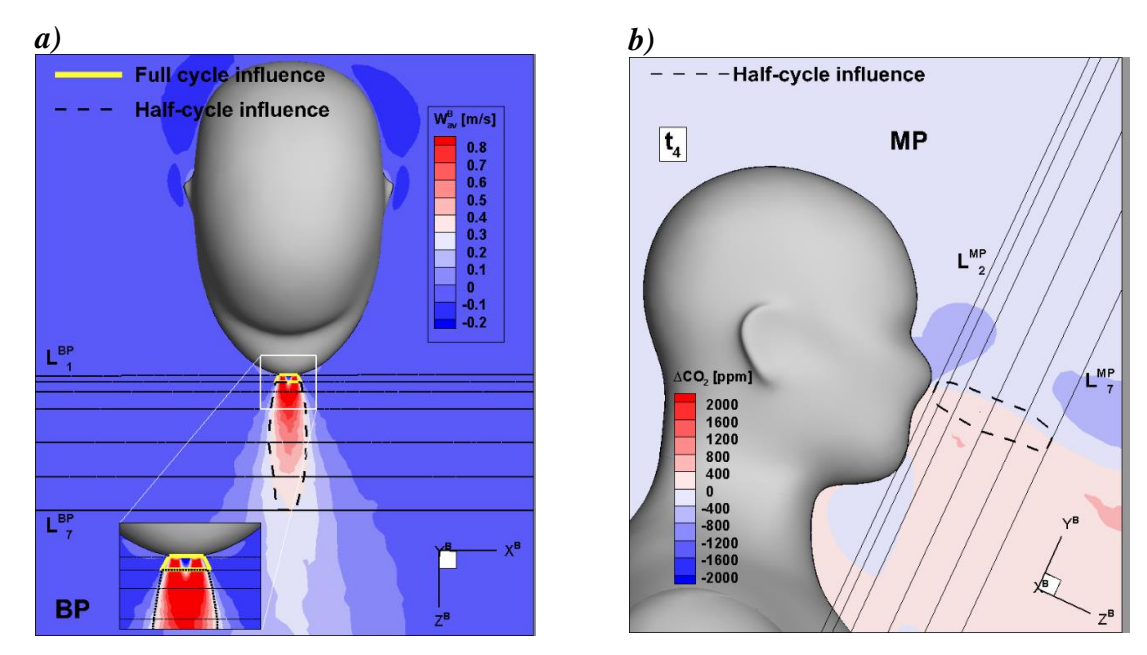


Figure 14 Reprezentation of the BZ in the BP superposed over a velocity field (a) and in the MP highlighting CO₂ accumulation in the BZ (b).

One of the most important accomplishments of the present chapter is the definition of the breathing zone by mathematical means. The BZ definition is important for the present thesis as it represents the chief region of interest for the ventilation study of the ISS CQ. The method's robustness evidenced by its seeming dismissal of perturbing environmental factors (the human convective boundary layer for example) highlights its potential and application in any domain interested in the identification and delimitation of a region of interest governed by strong periodic flows.

II. Modeling of the current ventilation solution and validation by experimental model at reduced scale

The second paper concerns the study of the CQ's ventilation system through numerical results obtained via CFD, validated with experimental PIV measurements. For the study of the ventilation a full-scale model of the CQ was designed. The ventilation circuits of the ISS CQ were reproduced to the best of the author's ability with the information available at the time. The ventilation system is powered by two axial fans in a serial connection. The ventilation circuit is quite intricate featuring multiple bends and turns, in the aim of equally distributing the air through the diffuser grille inside the CQ.

No velocity flow fields of the interior CQ airflow are available and the size and design of the full-scale CQ model prohibits high resolution PIV measurements at its interior. The was solved by simulating the CQ airflow numerically and then validating it with experimental PIV results in a transparent reduced-scale model.

The full-scale CQ model was built out of Oriented Strand Boards, connected with screws (Figure 15a). The axial fans as well as the ventilation ducts were all housed in the bump-out of the CQ (a detachable module around the CQ access point) (Figure 15b). Both the CQ interior (Figure 15c) and the interior of the ventilation ducts were subsequently covered in soundproofing materials.

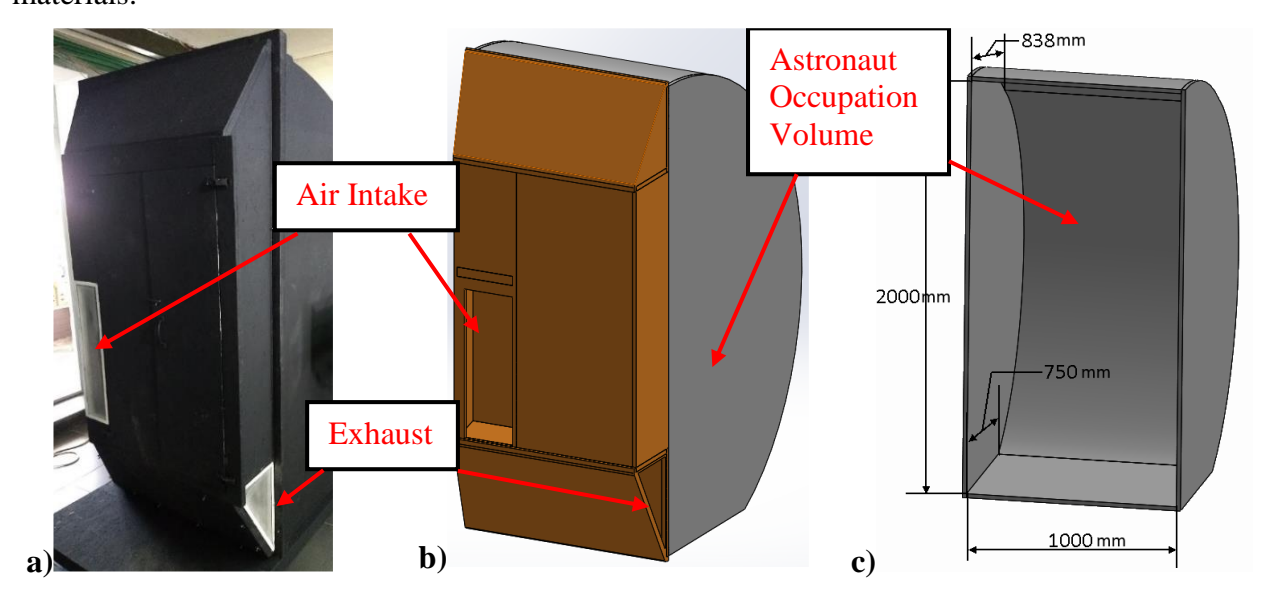


Figure 15 Full-scale CQ model in the laboratory (a), 3D representation the housing of the ventilation ducts highlighted (b), internal CQ volume (c).

Based on this full-scale experimental replica of the CQ, a numerical full-scale counterpart was designed with a numerical grid of ~5.5 million cells and 6 cells in the boundary layer near the walls. The fans and their circuits were included in the numerical model as well. The fan operating curves were measured experimentally in order to enable their use as a boundary condition in the numerical model.

An experimental setup was designed which allowed measuring the axial fan's rotation speed and pressure head as a function of different flow rates. Flow rates were controlled by varying

the diameter of the circular exhaust outlet. Velocities were measured along the diameter of the outlet, horizontally and vertically (Figure 16a). Results show little difference between the vertical and horizontal measurements, indicating a mostly uniform exhaust airflow. By integrating the velocity profiles over the circular surface of the orifice (via the trapezoidal rule) the flow rate was determined for each outlet diameter. The fan operating curve is obtained by plotting the fan pressure head as a function of its flow rate as seen in Figure 16b. The fan was powered by 24V direct current which was its nominal value.

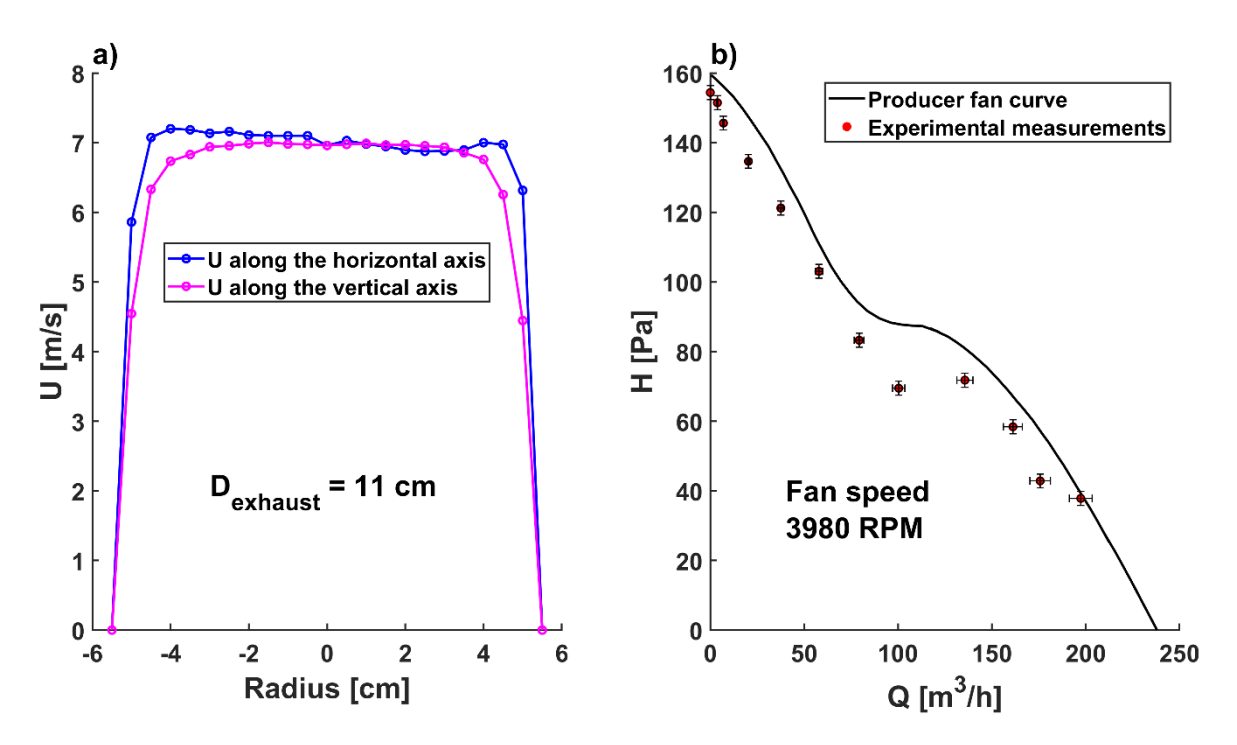


Figure 16 Streamwise velocity profiles along the horizontal and vertical of the circular outlet for D_{outlet}=11 cm (a), comparison between the measured operating curve and the producer's fan curve (b).

When placed inside an installation, depending on the head losses along the ventilation circuit the fan stabilizes itself at a certain flow rate and pressure head found along its operating curve. This is called the fan's duty point and it varies either according to the ventilation circuit's resistance or based on the fan's rotation speed. Introducing the operating curve as a fan boundary condition in the full-scale numerical model, simulates this process and the flow rate through the numerical model eventually stabilises itself at the fan's duty point. In the present case for a fan rotation speed of ~4000 rpm the flow rate through the CQ was 114 m³/h.

If we wish to change the flow rate through the numerical model, we must change the rotation speed of the fan. In order to determine the correct rotation speed for our desired flow rate the turbomachine affinity laws are used, namely the following formula:

$$\frac{Q_1}{n_1} = \frac{Q_2}{n_2} \tag{1}$$

Where Q represents the flow rate [m³/h] and n represent the fan rotation speed [rpm].

An experimental reduced-scale (1:4) model of the CQ was constructed out of acrylic. Correspondence between the flow fields of the reduced-scale model and the ones in the full-scale

model can be established provided the two operate at the same Reynolds number. Because of the reduction in scale, measuring airflow in the reduced scale model would demand velocities four times as high. For this reason, water was chosen as the fluid in the reduced-scale model. The difference in viscosity between water and air means that in order to obtain the same Reynolds number velocities in the reduced scale need to be three times lower than in the full-scale model, which is much more easily achieved.

In the reduced-scale model the flow rate was measured with an ultrasonic flowmeter. A 3D-printed realistic human model (down to scale) was placed inside the CQ in order to account for the occupant's influence on the flow inside the CQ. Velocity fields were investigated by PIV techniques in five planes around the diffuser grille. The positions of these planes along normalized axes can be seen in Figure 17. The flow rate through the reduced-scale model was 2.1 m³/h, resulting in a diffuser grille Reynolds number of 14000 placing it squarely in the turbulent regime.

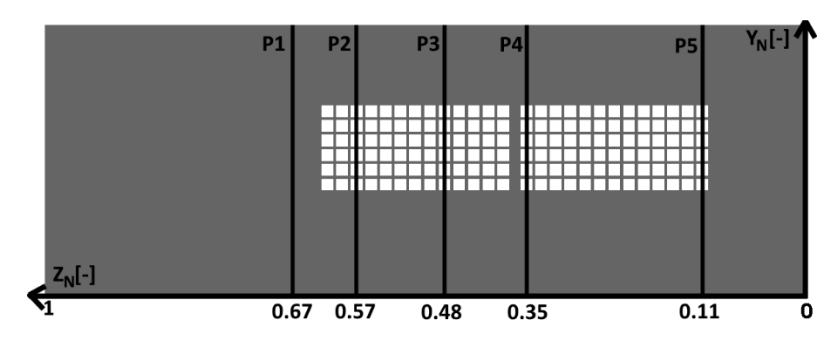


Figure 17 Interior view of the diffuser grille with highlights of the planes in which velocities were measured by PIV methods (P1-P5)

Because the aim is to validate the numerical results with experimental flow fields, in our case the desired flow rate for the CFD model will be the one which would generate a Reynolds number at the diffuser grille of Re=14000, just as in the experimental reduced-scale model. The airflow rate which results in this Reynolds number is ~134 m³/h, a value close to the intermediary flow rate of the ISS fans (138 m³/h).

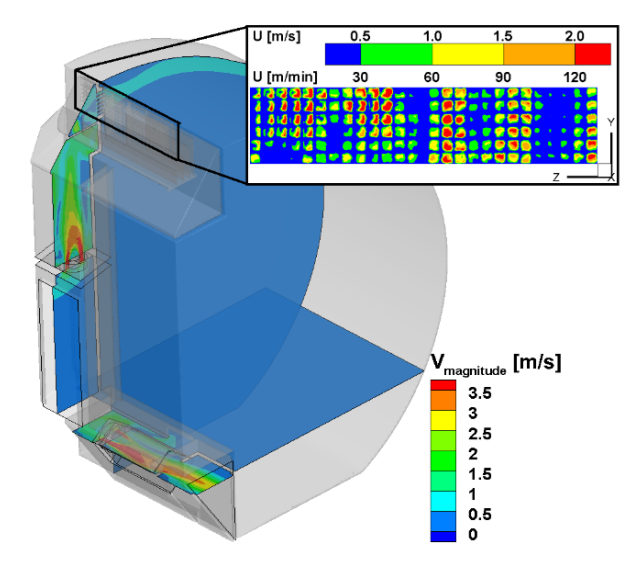


Figure 18 Median planes of the fans in the full-scale numerical model with a snapshot of the velocity

To obtain 134 m³/h in the numerical model, following the affinity laws the rotation speed required from the axial fan is ~4700 rpm. After calibrating the operating curve boundary condition in the numerical model, the velocity distribution across the diffuser grille was investigated and found qualitatively similar to other reports from the ISS CQ.

In order to properly compare the velocity flow fields between the two cases, a human model needs to be introduced inside the virtual CQ model. This has proved challenging as the realistic geometry of the virtual human requires considerable computational resources. Computational capabilities are already hampered by the complex ventilation circuit. It was thus decided to split the problem in two, and design a simplified numerical CQ model, comprised only of the CQ's internal volume (lacking the ventilation circuit) with the virtual human inside. The simplified numerical model has a numerical grid of 3.5 million polyhedral cells with 5 cells in the boundary layer near the walls and denser mesh regions around the human occupant. The boundary condition for this simplified model will be the velocity distribution across the diffuser grille which was previously extracted from the numerical model simulating the fans.

The numerical results from the simplified CQ CFD model were compared to PIV flow fields in the planes previously shown in Figure 17. An example of the comparison between the two cases in close proximity to the top wall is shown in Figure 19 in plane P4. In this figure the velocity of the PIV measurements was scaled to the levels of the full-scale model for comparison purposes. We see a recirculation region forming in both cases. The only difference between them is the attachment point of the ventilation jet to the wall, which is slower in the numerical results than in the PIV results. This is attributed to the difficulty of capturing accurate flow fields near walls.

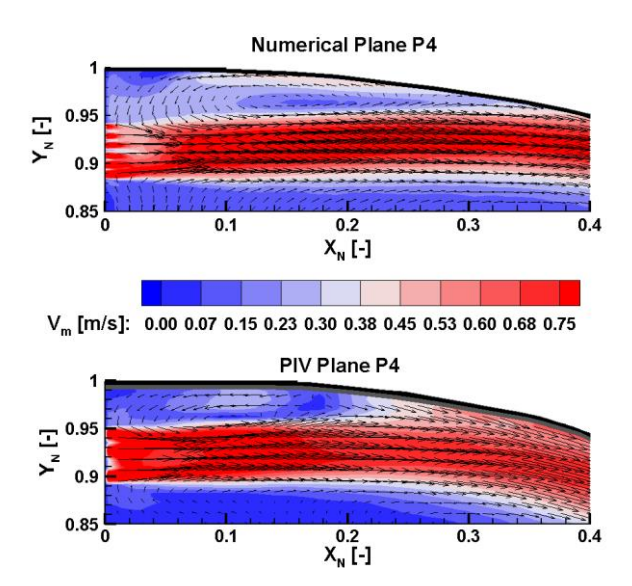


Figure 19 Flow fields in plane P4 highlighting a recirculation region near the diffuser grille

For a more general comparison of the flow dynamics between the two cases, several velocity profiles were extracted from the PIV (Figure 20a) and Numerical (Figure 20b) results in all of the measurement planes. These velocity profiles were superposed in Figure 21 for planes P1-P5. Their order follows the trajectory of the ventilation jet, keeping the colour code of Figure 20.

Globally the flow patterns of the two cases (PIV and Numerical) are in agreement, presenting only minor differences (Figure 21). Considering the numerical techniques used thus far valid, the three flow rate settings of the ISS axial fans (108, 138 and 156 m³/h) were investigated numerically. The results showed that the attachment of the ventilation jet to the curves wall is present in all cases, giving rise to a stagnation zone in the central area of the CQ. The increase in flow rate appeared to have minimal effect on the ventilation of this zone (velocity values below 0.2 m/s in all cases).

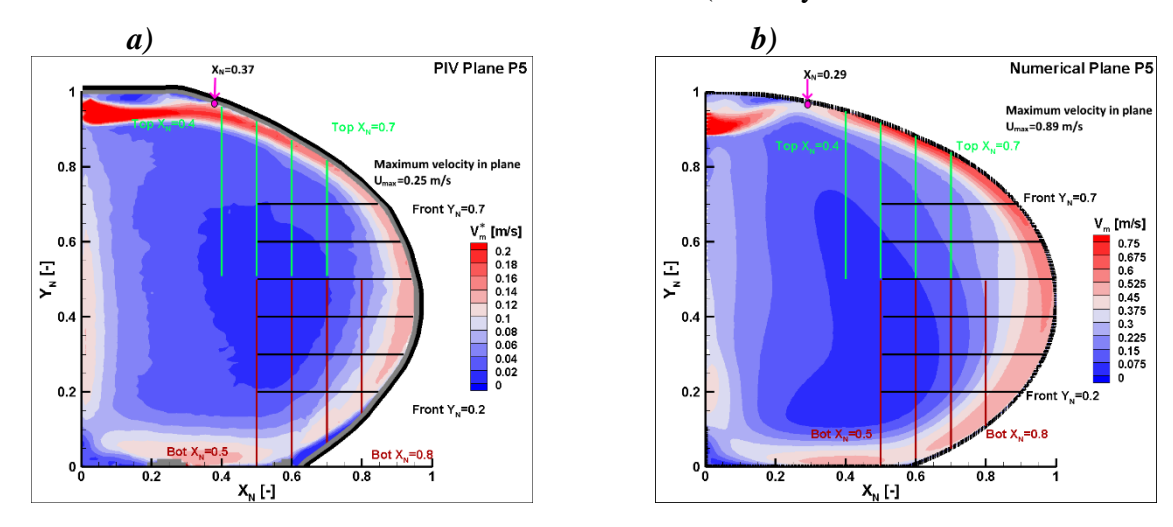
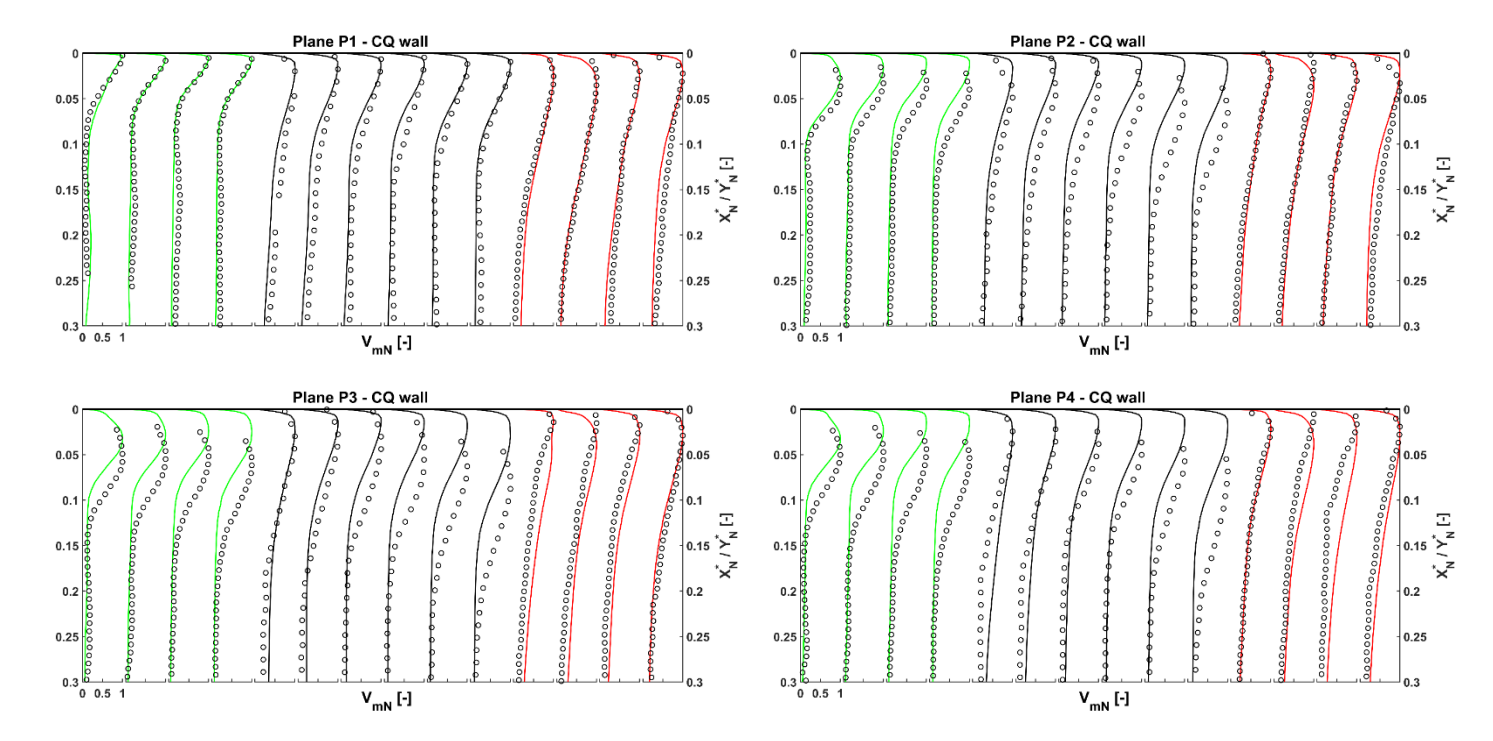


Figure 20 Locations of extracted velocity profiles from plane P5 in the experimental PIV (a) and numerical (b) cases



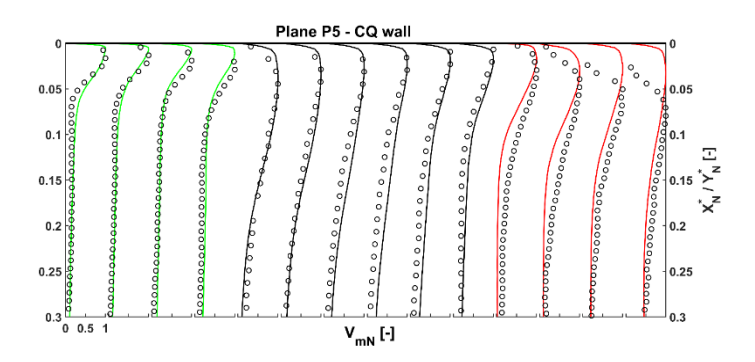


Figure 21 Normalized velocity profiles in planes P1-P5, following X_N or Y_N depending on the extracted profile's position (see Figure 20) – numerical data was represented with solid lines and experimental PIV data with black circles

Knowing that the flow rate has minimal impact on the stagnant air region inside the CQ, the region of CO₂ accumulation from the previous study was superposed over the velocity fields in plane P4 for comparison (Figure 22) and it was found that the ventilation jet does not directly affect this region raising the probability of CO₂ accumulation increasing in the occupant's BZ.

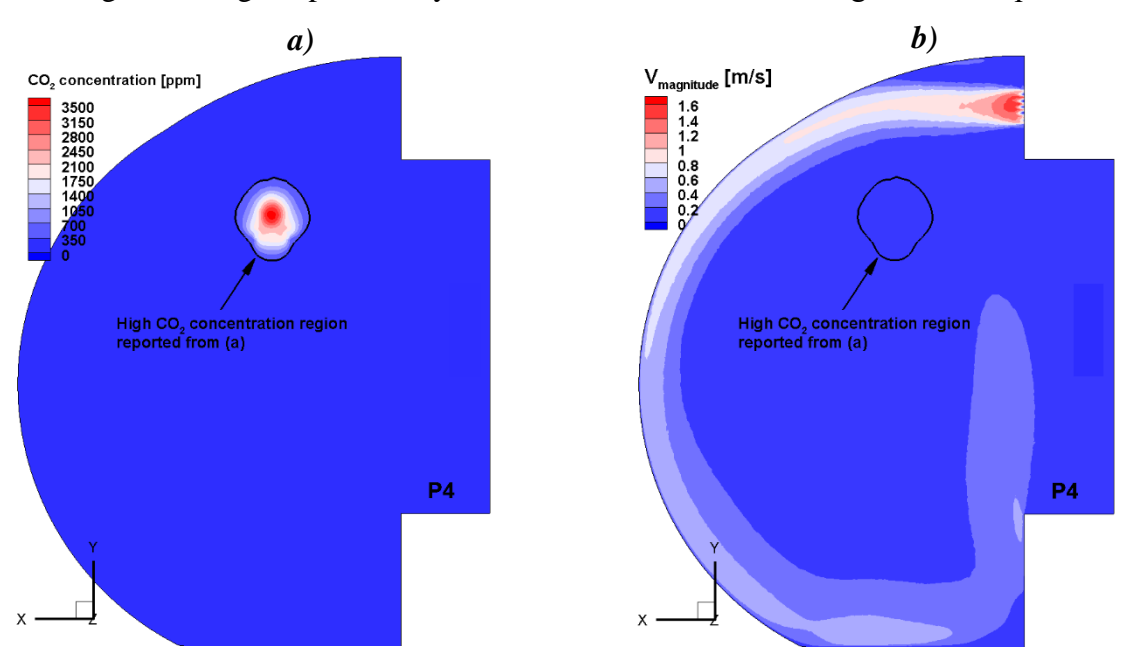


Figure 22 CO₂ concentration in front of the BZ (a) superposed over the velocity magnitude fields in P4 (b).

The results so far confirmed the suspicion that the BZ is not properly ventilated and that this is the reason for the CQ occupants' complaints. As a result of this study, it became clear that simply replacing the axial fans and the ventilation circuit might not sufficiently reduce the stagnation region seen in the flow fields. While improving the ventilation circuit is desirable there is a high likelihood that the BZ of the occupant needs to be locally ventilated in order to improve inhaled air quality.

III. Proposal for an improved general ventilation solution for better air diffusion and noise reduction

The present paper studies the impact of replacing the axial fan (AF) ventilation circuit of the CQ with a new circuit using cross-flow fans (CFF). The study uses the experimental and numerical methodologies which were successfully validated in the previous chapter. Fan operating curves will be experimentally measured and imposed in CFD models reproducing the CQ and each of the ventilation circuits. Flow fields will then be investigated. In addition, an experimental evaluation of the CFF acoustic performance will be undertaken and compared to the AF configuration as well as with results from the CQ's design process.

The experimental setup used to measure the CFF's operating curve is the one described in the first chapter of the thesis as well as in the previous paper, with the exception that the AF was substituted for the CFF. In a similar manner, the pressure head was measured, alongside the CFF's rotation speed and velocity profiles were integrated across the outlet to calculate the different flow rates. The CFF model chosen was powered by 24V DC (its nominal parameters). The operating curve of the CFF can be seen alongside the one for the AF in Figure 23.

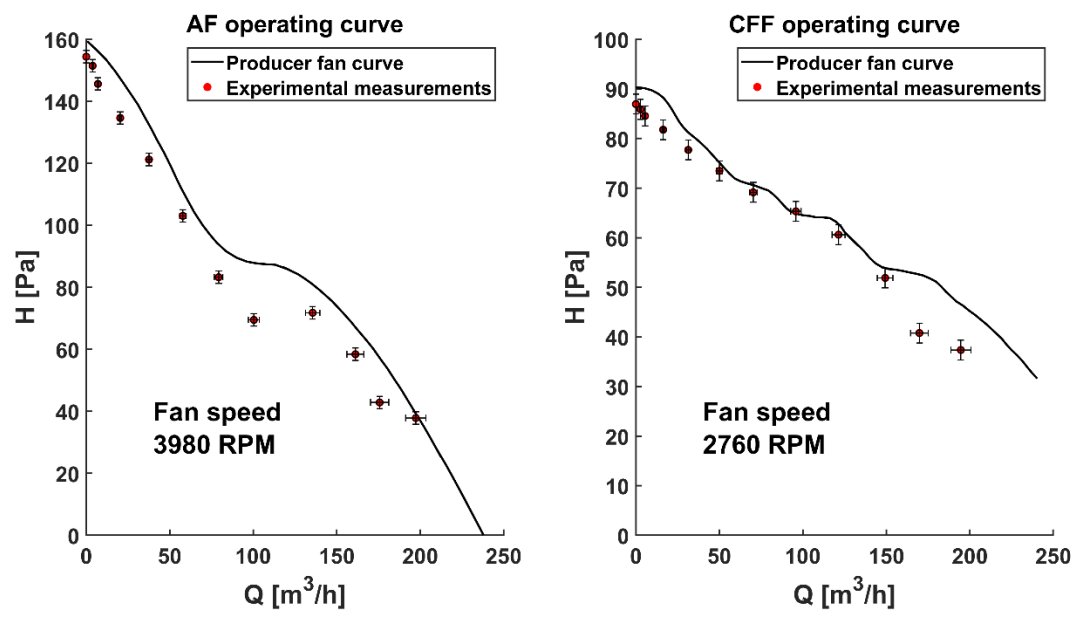


Figure 23 Operating curves of the AF and the CFF – comparison between the experimental measurements and the producer's information (AF: https://img.ebmpapst.com/products/grafik/7022-GRAFIK-GR.png and CFF: https://catalog.orientalmotor.com/Asset/mfd930-air.jpg).

Similar to the previous paper, the operating curve was imposed as a boundary condition in the numerical model of the CFF solution and the flow through the CQ stabilized itself at $181 \text{ m}^3/\text{h}$ at a rotation speed of ~2800 rpm. This highlights one of the major advantages of the CFF system. We recall that initially the AF operating curve at ~4000 rpm generated a flow rate of $114 \text{ m}^3/\text{h}$. The results clearly show that the CFF is able to provide higher flow rates at nominal parameters.

The efficiency of the axial fan at nominal flow rate and rotation speed is η_{AF} =21.2% while for the CFF η_{CFF} =16.4%. Small fans running on continuous current rarely have a good efficiency. In our particular case a more important factor than the efficiency is the fan's power draw.

Following the turbomachine affinity laws, fan rotation speed is directly proportional to the flow rate. For a required flow rate of 138 m³/h (the medium setting of the ISS CQ ventilation), for the AF case, because the initial flow rate (114 m³/h) is less than the required flow rate, the rotation speed n_{AF} must increase, thereby increasing the power draw. In the CFF case, the opposite happens: because the initial flow rate is 181 m³/h, obtaining the required flow rate implies decreasing the fan rotation speed and thus the power draw. The consequence of these facts is that the CFF consumes less energy overall.

The numerical procedure for the CFF study is the same as the one for the AF study. Two numerical models were designed (with computational domains around 3 million polyhedral cells). The first one had the entire ventilation circuit and used the CFF boundary condition calibrated for a flow rate of 134 m³/h (the value which resulted in a Reynolds number of 14 000 at the diffuser grille, the same Re as used in the PIV study). The second numerical model will be a simplified model which will use the velocity profile on the diffuser grille from the first numerical model as a boundary condition. The simplified numerical model will contain a virtual human inside the CQ.

Velocity distributions across the diffuser inlet between the AF and CFF cases were investigated to verify the hypothesis that the CFF would supply a more uniform flow rate. Additionally, the AF velocity distribution was compared to the results from the ISS CQ. The comparison of the diffuser velocity distributions is shown in Figure 24.

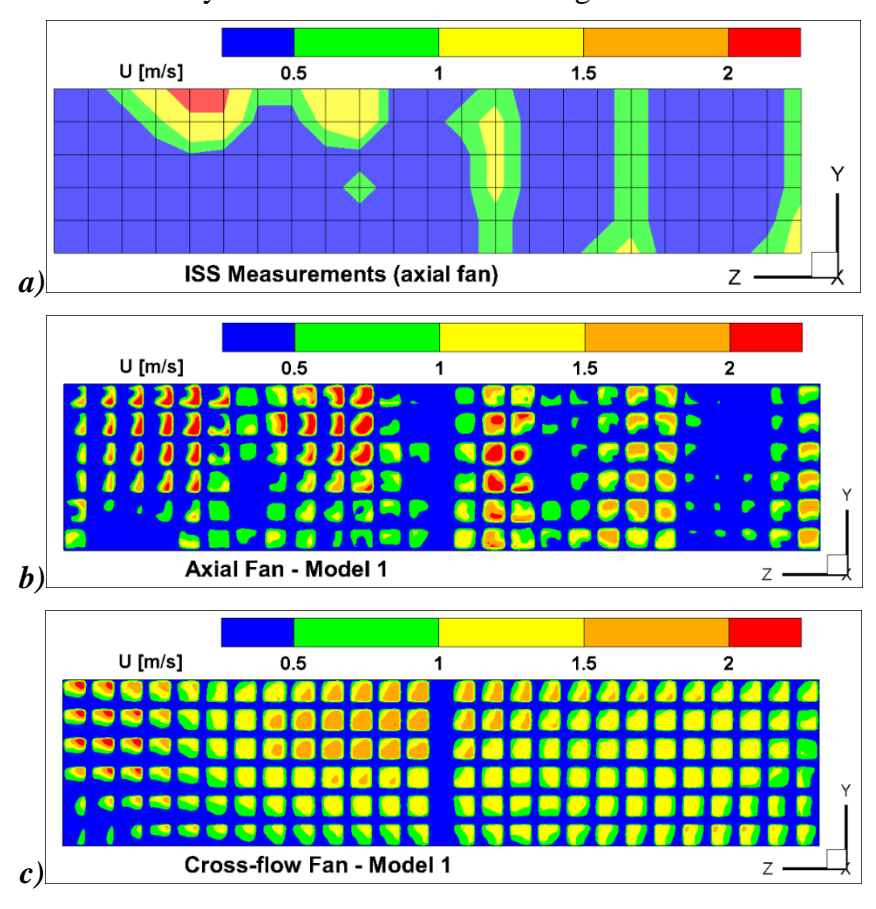


Figure 24 Streamwise velocity (U) distributions across the diffuser grille as measured in the ISS CQ (a) and simulated in the AF (b) and CFF models (c)

The ISS CQ measurements (Figure 24a) and the simulated AF results (Figure 24b) measurements compare well in a qualitative sense. Increased velocities can be seen in Figure 24a and b around the guiding vanes behind the diffuser grille. The guiding vanes were supposed to evenly distribute the flow across the diffuser, but it seems that the flow through the channels remains attached to the vanes. The CFF solution (Figure 24c) presents an almost uniform flow across the diffuser, with the exception of the bottom left corner, confirming the theory of a more uniform distribution. This is aided by the fact that the guiding vanes are not present in the CFF ventilation circuit.

A comparison of the flow fields in the AF and CFF cases revealed that the change in fan did not significantly alter the air distribution in the CQ. The stagnation region in the center of the CQ volume is still present. The CFF ventilation jet still attaches itself to the curved wall, albeit in a more uniform manner and with greater expansion than the AF case.

The acoustic performance of the CFF solution was also evaluated. Experimental measurements were undertaken in the full-scale CQ in three points situated around the head of the occupant and the diffuser grille. The experimental setup was designed in a similar manner to the one used for measuring the acoustic performance in the ISS CQ during its design.

Three microphones (Mic1-Mic3) recorded sound pressure levels at different frequencies between 63 and 8000 Hz. Experimental measurements were carried out at night, in order to diminish background noise levels. Two corrections were applied to the noise level measurements: a background noise correction (K1) and an environmental correction (K2) which accounts for reflected noise.

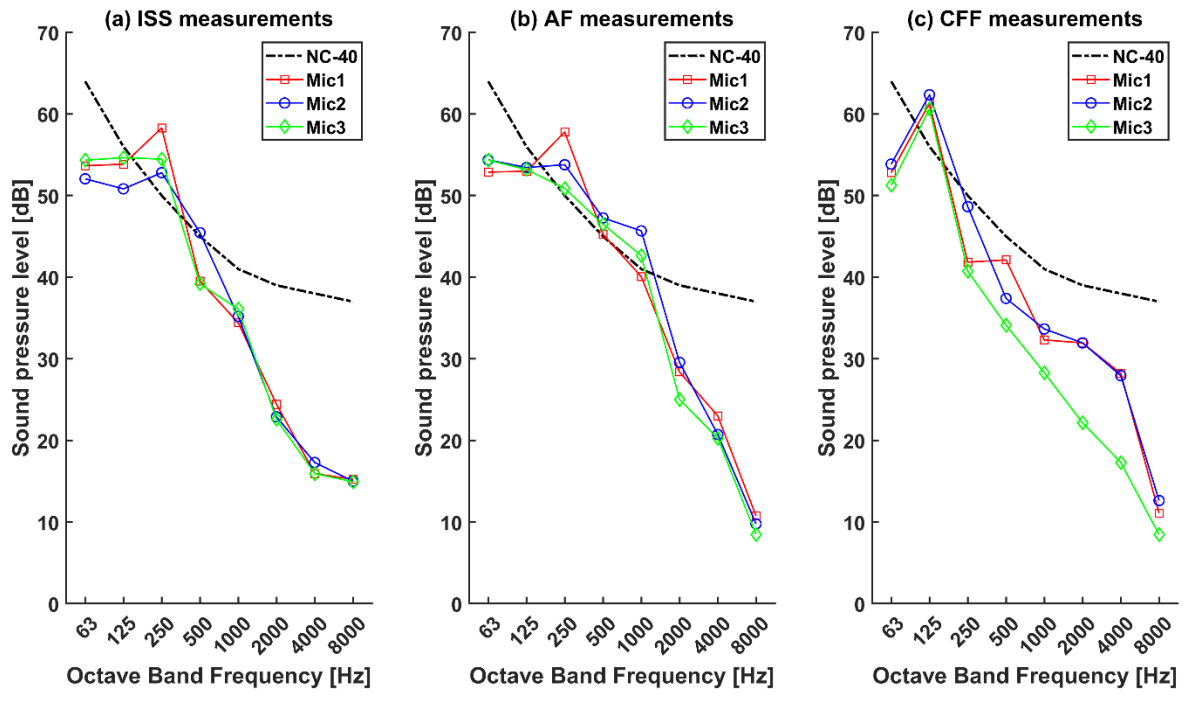


Figure 25 CQ design sound pressure measurements (a) compared to the experimental measurements obtained in the AF (b) and CFF (c) cases.

A comparison of sound pressure levels at different frequencies was studied for three cases: the measurements from the CQ's design phase (Figure 25a), the measurements of the AF solution in our full-scale CQ model (Figure 25b) and the measurements of the CFF solution (Figure 25c). In the graph corresponding to each case the noise criterion NC-40 curve was draw. We recall that sound pressure levels should be kept below this limit.

Figure 25 shows a tendency for all solutions to exceed the NC-40 curve at low frequencies. To help interpret the results we use the notion of "equal loudness curves". Equal loudness curves are plots of what level of sound pressure is required at different frequencies for the "noise level" to remain constant. These curves place peak human sensitivity in the 250 - 1000 Hz range. All of the solutions occasionally surpassed the NC-40 curve, but out of the three cases the one using a CFF solution is at an advantage because the human body perceives less noise at low frequencies, and the CFF solution only surpasses the NC-40 curve at values of 125 dB.

Considering the results of the present paper, we conclude that the CFF solution offers better airflow performance than its axial counterpart. The CQ weight can be reduced by the removal of the ducts is also an important aspect. From an electrical point of view, the CFF solution requires less power draw to offer the same performance as the axial fan. Sound pressure evaluations concluded that the CFF is an improvement over the AF solution despite the small number of points in which the NC-40 curve was omitted. The stagnation zone in the center of the CQ volume however, was not addressed by the CFF solution.

CFF systems are still recommended because of the CFF's superior parameters. In order to remove CO_2 from the CQ occupant's breathing zone simply installing a CFF solution is insufficient. To this end the following paper will cover the design of a personalized ventilation solution aimed at the occupant's breathing zone.

IV. Proposal for a complementary custom ventilation system to dilute carbon dioxide in the breathing zone

The final paper of the thesis studies the possibility of implementing a personalized ventilation (PV) solution to locally ventilate the BZ of the CQ occupant. The solution should be easy to implement from a technical point of view, and should avoid adding complexity to the ventilation circuit of the CQ due to the already existing limitations (e.g., power supply, lack of physical space and the requirement of two fans mounted in series to mitigate risks). An easy answer to the above requirements is to design the PV circuit to be passively supplied by the same fans that power the general ventilation inside the CQ. This would require no additional power draw, would benefit from a safety measure in the sense that it is powered by two fans, and the only limitation would be available physical space, so it is desirable for the solution to be compact.

Following the state-of-the-art study of PV systems presented in the first chapter of the thesis, the decision was made to implement a lobed PV diffuser with an equivalent diameter D_e =3 cm, at a distance of 6 cm $(2D_e)$ from the nose of the human occupant. We recall that this configuration was chosen because of the lobed diffuser's capabilities to offer better initial spread without reducing the jet's throw length.

The study of the PV system was done through CFD. For this reason, experimental validation of the numerical results was required. The experimental setup used to measure the CFF operating curve was repurposed. A duct supplying the PV diffuser with air was installed, with a flow meter connected half way along it. Opposite the PV diffuser a human manikin was placed on a chair in the laboratory at a distance of 6 cm between the manikin's nose and the lobed PV diffuser. Velocity flow fields of the PV jet were measured with a hot-sphere anemometer in planes perpendicular to the PV diffuser's axis.

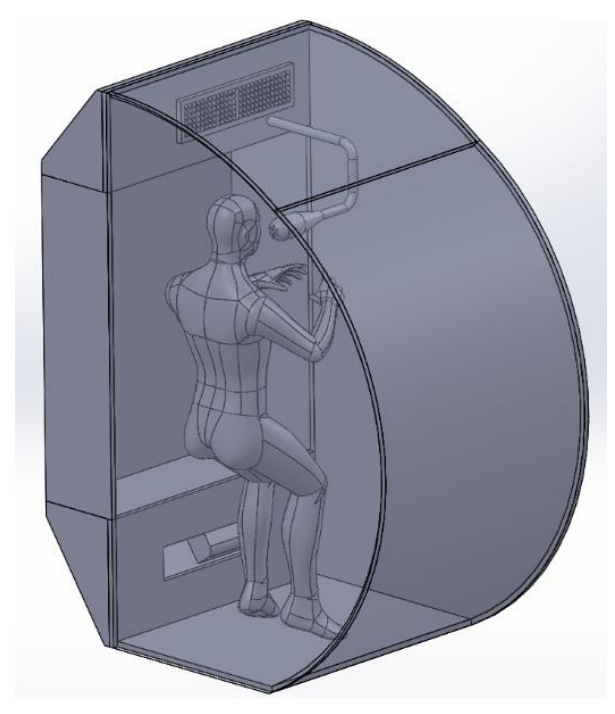


Figure 26 Interior view of the CQ with the virtual human occupant inside and the frontal PV diffuser

A numerical model was designed of the PV system implemented in the CQ installed in front of the virtual occupant at a distance of 6 cm as seen in Figure 26. The numerical results were obtained following the procedure outlined in the previous papers: the first numerical model was powered by the CFF and velocity profiles were used as boundary conditions in the second simplified model which contained the virtual human occupant. Because this study will make extensive use of numerical models with different ventilation configurations the following naming scheme was designed: models using the fan operating curve as boundary conditions are dubbed Ventilation Models (VM) and the simplified models using velocity profiles as boundary conditions are called Simplified Models (SM). The ventilation configuration is represented by a number: 1 corresponds to the CFF solution and 2 corresponds to the frontal PV solution. In the images in the paper the above naming scheme will be used in photos to represent the case in question (e.g., SM2 for the simplified frontal PV case).

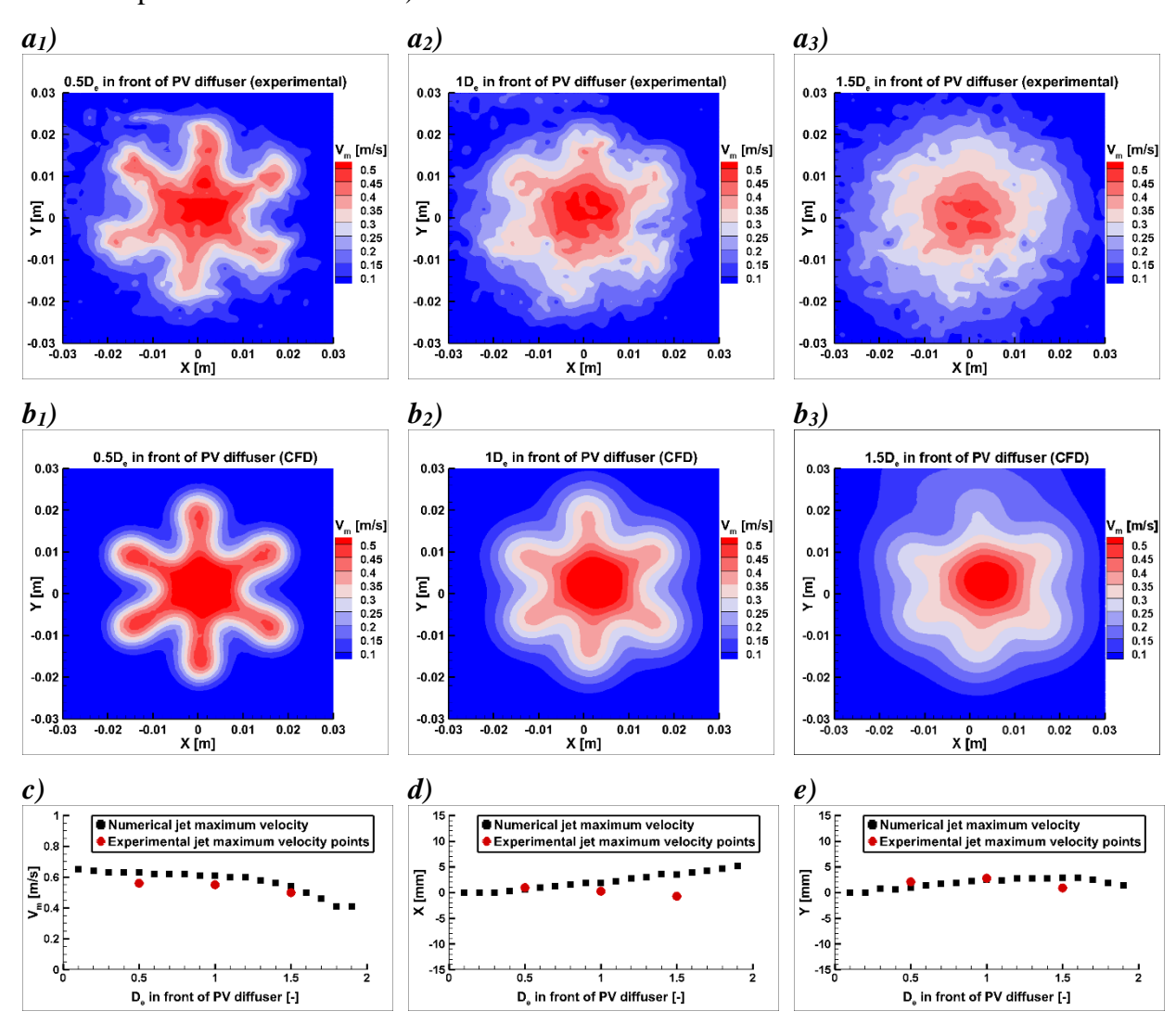


Figure 27 Validation of the experimental (a) and numerical (b) PV system: velocity magnitude at 0.5D_e (1), 1D_e (2), 1.5D_e (3); PV jet velocity decay along the Z axis (c); PV jet trajectory along the X (d) and Y (e)

A simulation was run in the simplified model of the frontal PV diffuser at the same flow rate as the one in the experimental measurements of the PV velocity profiles (1.2 m³/h) for validation purposes. The validation was done at different distances between the PV diffuser and the occupant's nose as seen in Figure 27.

In Figure 27 the lobed form of the jet is well defined at $0.5D_e$, with remnants still present at $1D_e$ up until around $1.5D_e$ when the remnants have all but dissipated. The numerical (Figure 27b) velocity fields are similar to the experimental results (Figure 27a), in both cases peak velocities are around 0.5 m/s. The maximum jet velocity plot (Figure 27c) shows the two results in accord, as does the jet trajectory along the Y axis (Figure 27e). The slight deviation found in Figure 27d is to be expected because of the symmetrical shape of the human face along the X axis, and anything less than perfect alignment between the PV diffuser and the face is bound to influence the jet's trajectory to the right or to the left of the face.

The CFD model was considered capable of representing the dispersion of the PV jet and so, a transient numerical simulation was run with the frontal PV system, the general ventilation in the CQ (through the diffuser grille) and the virtual human breath simulated through the realistic breathing function designed in the first paper of the thesis. The results (Figure 28) indicate that at the end of the exhalation phase, the proximity between the virtual human and the PV diffuser led to the contamination of the air inside the diffuser with CO₂. This was caused by the exhaled flow having higher velocities than the PV flow, causing it to enter the diffuser. At the end of the inhalation phase, it was found that the CO₂ introduced in the diffuser had not been completely evacuated and so, the decision was made to alter the PV configuration as the frontal PV solution proved unfeasible.

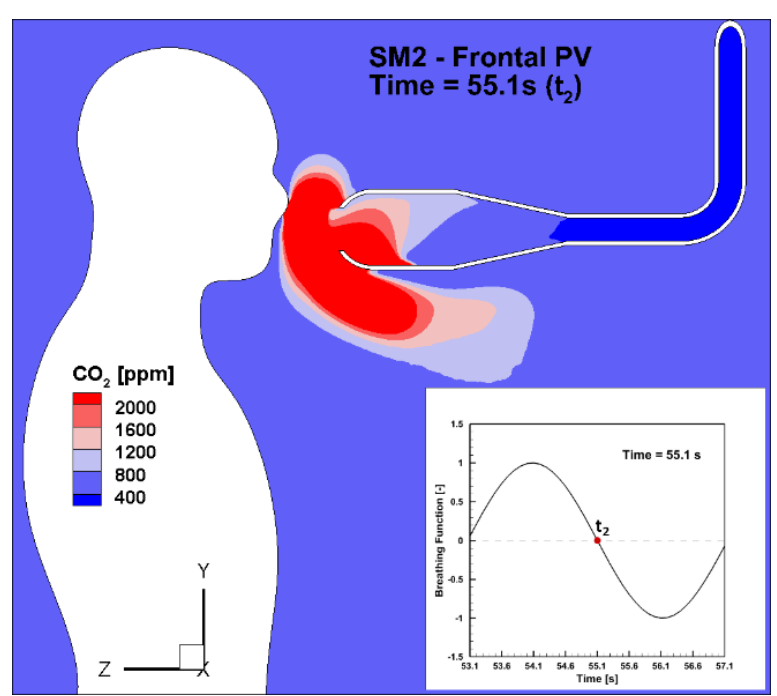
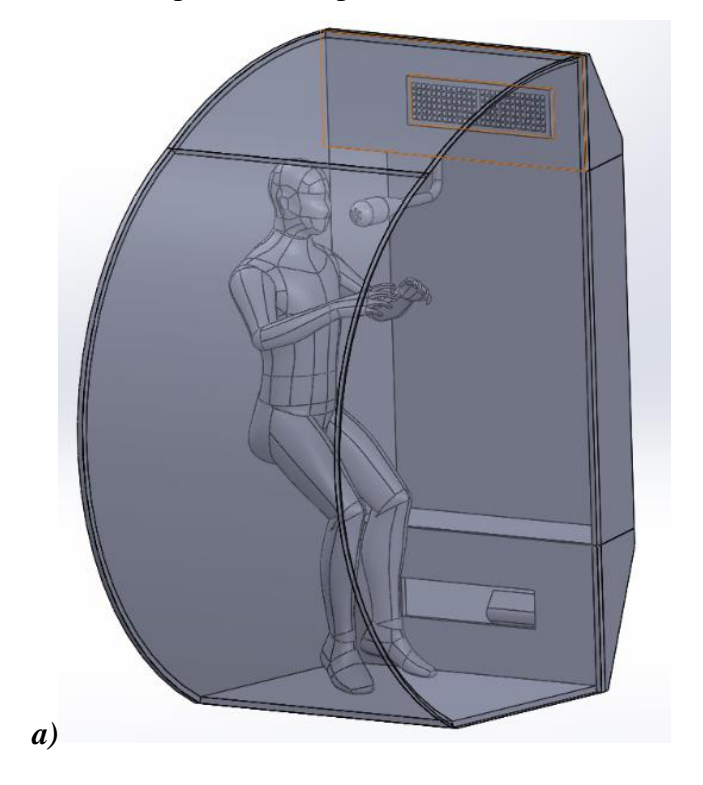


Figure 28 Interaction between the frontal PV diffuser and the human breath at the start of inhalation (t2).

An alternative PV solution was implemented (VM3 and SM3), with the lobed diffuser to the left of the human occupant's head, targeted on the nose and the mouth area (Figure 29a). The same distance of 6 cm was kept between the diffuser and the human face. The idea behind this

solution was to have the PV jet displace the exhaled air towards the general ventilation jet which travels along the curved wall as was evidenced in the previous paper of the thesis. Because the air would be naturally entrained in the direction of the general ventilation jet, there would be little risk of the diffuser becoming contaminated with CO₂ as it did with the frontal PV configuration. The change in position from the frontal to the lateral PV emplacement caused a change in flow distribution inside the plenum. More flow entered the CQ from the lateral PV (3 m³/h) than from the frontal configuration (1 m³/h) due to lower head losses along the circuit. Consequently, the increase in PV flow was followed by a decrease in diffuser grille flow. Because the aim is to compare the systems between one another it was decided to reduce the lateral PV flow rate by introducing head losses along its circuit, numerically represented by a porous media inside the horizontal PV duct leading up to the diffuser. The CFD software does not physically model obstacles when setting a porous media, instead it reduces the magnitude of the velocity vectors passing through it, while keeping their direction – essentially altering the flow rate without changing its distribution. Moving forward the impact of the lateral PV solution will be evaluated by comparison with regular ventilation conditions using the CFF. This comparison will take place in several representative planes for the CQ ventilation shown in (Figure 29b).



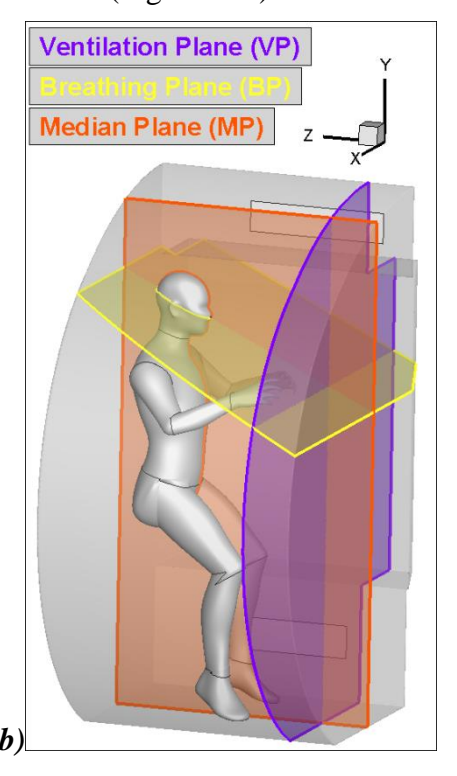


Figure 29 Interior view of the CQ with the virtual human occupant inside and the lateral PV diffuser (a); representative CQ planes for the investigation of the CFF and lateral PV configurations

Because the PV solution exhausts air in very close proximity to the occupant's face it is important to make sure that generating an uncomfortable sensation of draft is avoided. The parameter used to evaluate this sensation is called the draft rate (DR [%]), and it represents the percentage of people which report a sensation of draft. The draft rate is computed with the following formula:

$$DR = (34 - T) \cdot (V_{avg} - 0.05)^{0.62} \cdot (0.37 \cdot V_{avg} \cdot T_u + 3.14)$$
 (1)

Where T is the local air temperature [°C]; V_{avg} is the average local velocity magnitude [m/s] and T_u is the local air turbulent intensity [%]. DR should be below 30% in all cases to avoid uncomfortable sensations. A comparison of DR between the lateral PV solution and the CFF solution is shown in Figure 30. Results show that unacceptable levels of DR are only found in the core of the general ventilation jet. The V solution generates draft rates between 10 and 30% in proximity to the face which makes the PV diffuser configuration acceptable for use.

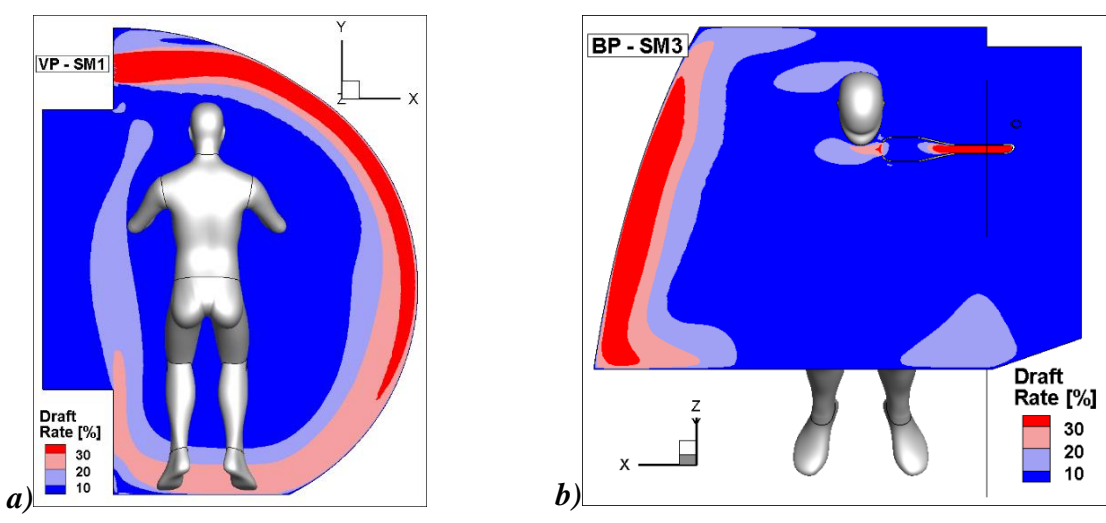


Figure 30 Draft rate evaluation of the CFF solution (a) and the lateral PV solution (c).

The average CO₂ accumulation in the CQ was found to have an increasing tendency for both the CFF and the lateral PV solution. The increase over the last 20 seconds of the simulation were of ~28 ppm for the CFF case and 25 ppm for the lateral PV case. These results indicate that the PV has a beneficial impact on the ventilation but is not sufficient to combat the accumulation on average in the entire interior volume of the CQ.

The following comparison between the CFF and lateral PV solutions concerns the CO_2 accumulation in the BZ (Figure 31). Recalling the results of the first paper, the BZ has two components: (1) the yellow region which is where the influence of both exhalation and inhalation can be felt; and (2) the region marked with a dashed black line, where the exhalation is predominant. The comparison was done at the same moment in time for both cases, namely the end of the exhalation in the breathing plane (BP - Figure $31a_1$ and b_1) and in the median plane (MP - Figure $31a_2$ and b_2).

The entrainment of the breathing jet towards the curved wall (the left side as seen in Figure $31a_1$ and b_1) is expected and attributed to the general ventilation jet. However, in Figure $31b_1$ the influence of the lateral PV solution is seen displacing the breathing jet further towards the curved wall. In Figure $31b_2$ this is all the more evident as we can see that the CO_2 concentrations hardly reach the midpoint of the BZ in the median plane.

A quantitative evaluation of the CO_2 content [ml] in the BZ over the course of a breathing cycle (exhalation + inhalation) revealed that peak CO_2 concentrations were 40% lower in the BZ when using the lateral PV rather than the general ventilation by itself. In addition, at the end of the

start of the inhalation CO₂ levels in the CQ were three times lower with the lateral PV than without it.

Initial and final values of CO_2 were practically identical, suggesting that at the end of the breathing cycle the air in the BZ was back at the average CO_2 level of the CQ. This seems like a good result, but previous results showed that the CO_2 accumulates in the CQ over time, driving the average concentration up. Computational resources limited the present study to just 60s, but over the course of multiple hours this increase could compound, reinforcing the usefulness of the PV system.

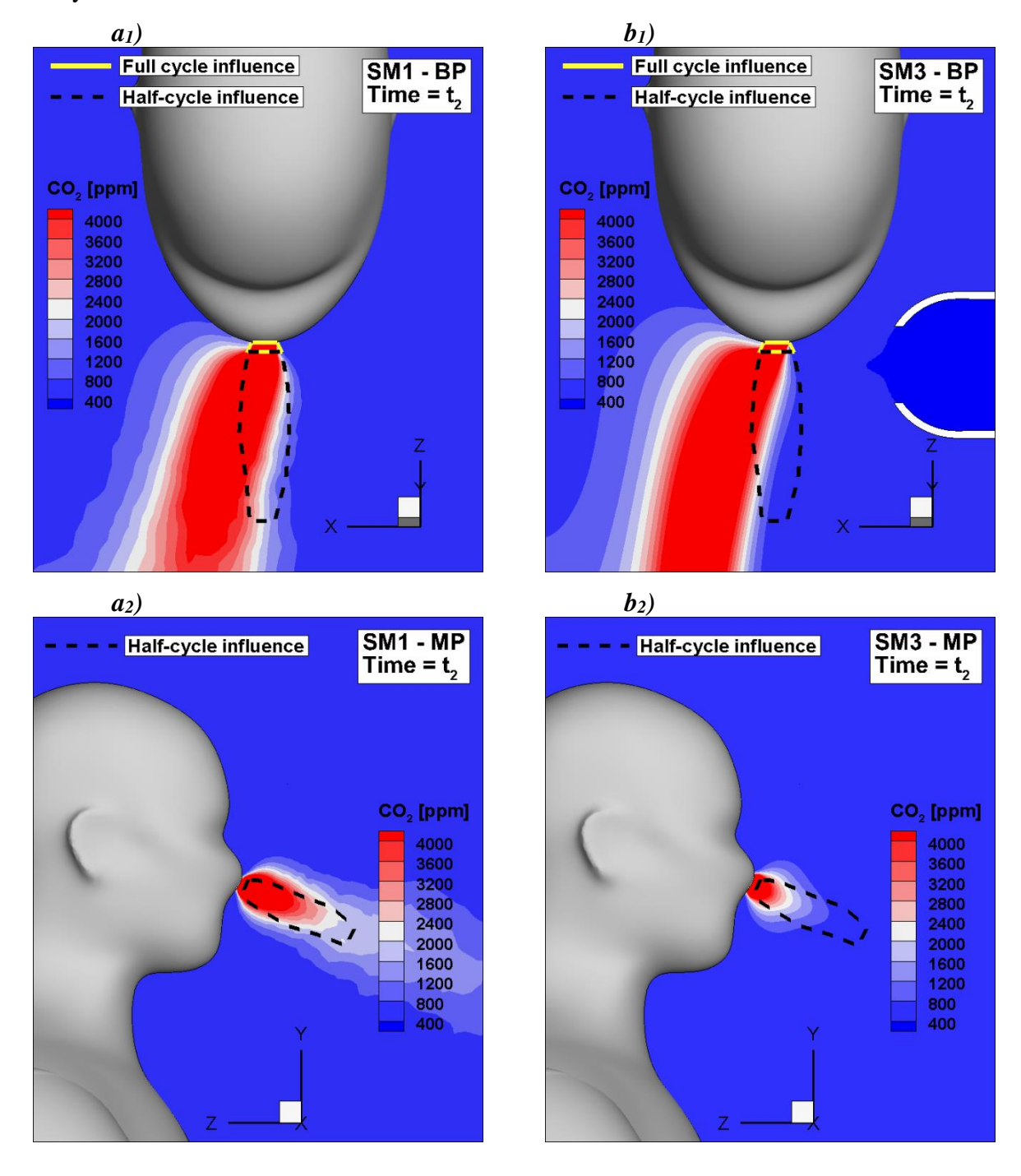


Figure 31 CO₂ accumulation in the BZ for the CFF (a) and lateral PV (b) cases in MP (1) and BP (2).

The final comparison of the paper is the numerical investigation of the volume of CO₂ inhaled during each breathing cycle (Figure 32). This volume can be calculated as follows:

$$InhaledCO_2 = Q_{nostrils} \cdot t_{step} \cdot VFCO_2$$
 (2)

Where InhaledCO₂ [ml] is the volume of inhaled CO₂, Q_{nostrils} [m³/s] is the flow rate through the nostrils, t_{step} [s] is the time step of the unsteady simulation and VFCO₂ [ppm] is the average CO₂ volume fraction across the nostrils. The results of Figure 32 indicate that although at the start of the inhalation the quantity of inhaled CO₂ is practically identical, by the end of the inhalation we find that when using the lateral PV system, ~8% less CO₂ is inhaled. Although this value might appear small, when taking into account the overall rise in CQ CO₂ levels, the 8% increase over each breath has the potential to become significant.

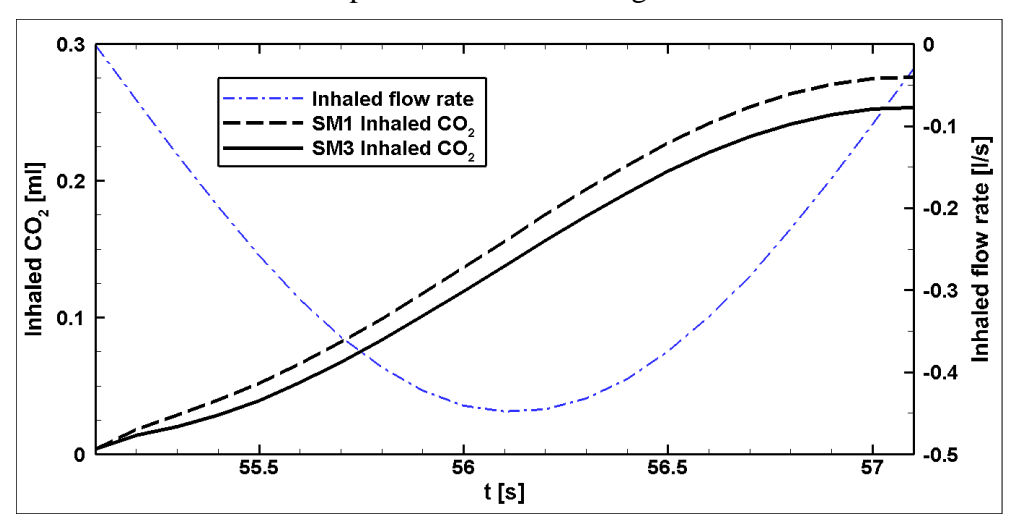


Figure 32 CO₂ inhaled during an inhalation (55.1-57.1s) for SM1 and SM3

Investigations of PV systems in the CQ revealed that the proposed PV solutions were easy to implement, passive in energy consumption and had no adverse impact on the global air distribution in the CQ, nor on the comfort sensation of the occupants. The frontal PV solution was discarded as it did not fulfill its objective. If a frontal emplacement of the diffuser is to be attempted in the future recommendations are to move the frontal diffuser further away from the face and increase the flow rate to compensate for the increase in distance. The lateral PV diffuser proved efficient showing significant reductions in CO₂ content in the breathing zone as well as an 8% reduction in inhaled CO₂ per breath. The PV solution was not able to combat the accumulation of CO₂ in the entire CQ volume, however, it is all the more valuable for this reason because of its potential to supply fresh air to the breathing zone despite the ever-increasing CO₂ levels in the CQ. Overall, there is little reason not to implement a PV solution given its ease of implementation and practically inexistant energy requirements.

Conclusion

The aim of the present thesis was the study and improvement of the ventilation system aboard the Crew Quarters installed on Node 2 of the International Space Station. The thesis was motivated by reports of occasional CO2 intoxication incidents aboard the ISS. CO2 is a more dangerous pollutant in space than it is on Earth, because in microgravity, without mass there is no convective flow of air due to temperature differences. Natural mixing happens only by molecular diffusion which is a comparatively slow process. In such conditions, if an enclosure is not properly ventilated a human occupant will generate a cloud of CO2 around the head increasing the risk of intoxication. This phenomenon is especially prevalent in confined spaces such as the CQ which the astronauts use for personal time and sleep during the "night". Preliminary investigations of the CQ ventilation system revealed a complex system needing to fulfill several requirements (flow parameters, energy efficiency, noise levels) at once. Problems reported related to insufficient CO₂ evacuation when the ventilation system was used on its lowest setting or acoustic discomfort at high fan speed settings, all point to the main culprit being the ventilation system. The plan to improve the ventilation system consists in simplifying the ventilation circuit, in most part by replacing the axial fans currently in use on the ISS with cross-flow fans which are quieter and provide better airflow parameters. The efficacy of the proposed solution will be evaluated by its ability to diminish CO₂ accumulation inside the CQ. Along the improvements to the general ventilation system, a personalized ventilation solution is proposed with the intention of targeting pockets of CO₂ if they form in poorly ventilated regions around the occupant's heads.

The first chapter contains a literature review of the environmental conditions aboard the ISS in order to better understand the core issue of the problem, followed by a literature review of the techniques and methods perceived as necessary to solve said problem. The state-of-the-art study revealed that a sum of factors contributes to the CO₂ accumulation issues. Firstly, the systems used on the ISS to scrub CO₂ from the air, cannot reduce CO₂ concentrations below a limit of ~3000 ppm for energy efficiency reasons, meaning that at best CO₂ levels aboard the ISS are almost 8 times greater than on Earth at sea level. Secondly, the ventilation circuit of the CQ is very complex and has considerable head losses as a result of a complex ducting system meant to evenly distribute the flow through the ventilation diffuser grille inside the CQ. This goal was not fully accomplished as although the flow was distributed through several channels, higher velocities were found near the directing vanes of the channels and large sections of the diffuser showed very low velocities. The head loss issue is further evidenced in reports stating that for the lowest fan setting, dust accumulation in the ventilation ducts leads to alarms being set off because of low flow rates through the fan. Lastly, numerous studies concerning the CO2's impact on astronaut health and performance unanimously concluded that there are significant variations in the personal tolerance of each crew member to CO₂ concentrations. No consensus was reached on a limit of CO₂ which above which intoxication effects occur and thus recommendations were to keep CO2 levels as low as possible.

The first chapter proceeds with a literature study concerning the mechanism of human CO₂ generation consulting multiple studies dealing with air quality as well as medical manuals. These studies revealed that human breathing is a very complex phenomenon to simulate in its entirety because of the numerous micro-adjustments made by the human body which are frequently unaccounted for and simulated by empirical means (i.e., equivalent quantity of CO₂ generated per day). One study numerically simulated CO₂ generation aboard the ISS in an old version of the CQ cabins and found significant accumulations but did so by representing the breath as a constant

stream of exhaled air. Most studies agreed that the dynamic nature of the breath is important and used sine-wave functions to represent the exhalation and the inhalation. The quality of the air surrounding a human occupant is frequently measured in the breathing zone. The literature study revealed numerous breathing zone definitions, most of them loosely based upon available experimental techniques and no clear consensus could be established.

Velocity flow fields of the air distribution inside the CQ were not found in the literature. For this reason, PIV methods in reduced scale models were studied in order to obtain experimental velocity fields which could be used to validate numerical results. A number of building ventilation studies were found measuring velocity fields in reduced-scale models of enclosures using water as the working fluid and equivalating them to results at the full-scale provided the latter used the same Reynolds number. The full-scale numerical methods can use experimentally measured fan curves to determine the flow rate through the CQ ventilation circuit. The fan operating curves were measured in experimental setups mimicking the ones used for the same purpose during the CQ design process. Additionally, acoustic requirements are that the sound pressure of the fans falls below the NC-40 curve. For this stage too experimental setup designs mimicked the ones used in the ISS CQ.

A proposal for a new ventilation circuit using cross-flow fans instead of axial ones was studied. CFFs are known in the literature to provide good flow parameters and good acoustic performance. The proposal was to replace the complex ventilation circuit of the CQ with a simplified version featuring a CFF placed in the plenums of the CQ, relying on pressure buildup inside the plenums to provide a uniform air distribution through the diffuser grille. In addition, the possibility of implementing a personalized ventilation solution was studied. Extensive research in the field of PV revealed that one of the biggest impediments on Earth is the convective boundary layer of the human body which must be penetrated by the jet in order to supply fresh air to the breathing zone, all without adverse effects on human comfort levels. This can be done by installing the PV diffuser close to the human, and by choosing diffuser geometries which help spread it out over a larger surface without negatively influencing its travel distance (such as lobed jets). It was decided to implement such a PV solution in the new CQ ventilation proposal.

The first paper concerns the study of CO₂ accumulation in the CQ from a phenomenological point of view (without other influencing factors such as the ventilation system). Experimental measurements of CO₂ accumulation were performed in a full-scale CQ model in our laboratory using multiple human test subjects. An average rate of CO₂ generation rate was determined based on these measurements. A sine-function of the breath was then devised so that it reproduced in a numerical full-scale CQ model the same average CO₂ levels as in the experimental results after a time interval of 60s. The results were in agreement and the first goal of simulating the human breath in a realistic manner was accomplished.

A major milestone of the thesis comes from the conception of a rigorous method for delimiting the BZ. Because the human breath is periodic in nature, this periodicity is numerically represented by the frequency of the sine-wave breathing function. Without the room being ventilated, and because in microgravity convective free flow does not exist, the only source of perturbation for the CQ air was the human's breath. The BZ by definition is influenced by the dynamics of the breath, so in order to delimit it a method was required to quantify the influence of the breath. The Fast-Fourier Transforms (FFTs) were used for this purpose as they evaluate the variation of a signal (in our case the velocity) in a point over time, and reveal the underlying frequencies of the signal's variation. By searching for the known breathing frequency, the BZ was

spatially defined and divided into two regions: the first where a strong influence of both the exhalation and the inhalation can be felt and a second where a weaker influence is felt or possibly (and very likely) only the exhalation part is predominant. The BZ thus defined will be used to evaluate the performance of the proposed ventilation solutions.

The second paper studies the flow distribution inside the CQ by validating numerical results of the full-scale CQ ventilation with experimental velocity-fields measured in a reduced-scale CQ model through PIV techniques. The similitude theory was used to establish a correspondence between the two different scales provided the Reynolds number is the same between the two cases. In the CFD model, the flow was simulated by imposing the fan operating curve as a boundary condition. The flow eventually stabilizes itself at the duty point along the operating curve. The flow rate can be changed by modifying the fan rotation speed (and consequently the operating curve) following the turbomachine affinity laws. This procedure was used in the present paper to ensure that the flow rate through the CFD model is the scaled equivalent of the one in the experimental study. The numerical velocity fields inside the full-scale CQ model compared well with the experimental PIV fields and the numerical model was considered successfully validated. Subsequent investigation of the velocity distributions inside the CQ revealed that there is a region of stagnant air in the center of the CQ. A comparison with numerical CO₂ accumulation results shows that the regions of high CO₂ concentration are found within that stagnant air region.

The third paper studied an improvement of the ventilation system by replacing the axial fans with cross-flow fans in a simplified version of the ventilation circuit. The same method of measuring the operating curve and using it as a boundary condition in the numerical model was used. Comparison of the flow fields inside the CQ showed little change from the results of the axial fan in terms of overall flow distribution. From an energy efficiency point of view the CFFs consumed less energy to supply the same flow parameters than the AFs did. Acoustically both CFF and AF configuration surpass the NC-40 curve with value of ~3dB at different frequencies. The CFF surpasses the curve at lower frequencies than the AF, and because the human ear is less sensitive to low frequencies it was considered that the CFF had superior acoustic performance. Despite the superior acoustic and energy performance of the CFF, because it does not fundamentally change the flow distribution inside the CQ, it is unlikely to perform better than the AF solution in regards to CO₂ removal from the occupant's breathing zone.

The Final paper of the thesis implements a personalized ventilation system inside the CQ. The PV system is connected to the upper plenum of the CQ and is supplied by the CFF ventilation system. The PV diffuser is to be installed opposite the occupant's face, targeting the BZ. Similar to the previous papers, experimental measurements of the PV system are required to validate the numerical results. Velocity flow fields were measured with a hot-sphere anemometer at different distances between the PV diffuser and the human occupant. The experimental velocity fields were compared to numerical results of the PV system at the same flow rate and the two were found to be in agreement. Upon investigation of the CO₂ accumulation, it was found that the PV diffuser was too close to the face and the exhaled air contaminated the diffuser's interior with CO₂, which could not be completely evacuated over the course of one breath. A second PV system was designed which had the diffuser installed to the side of the human face at the same distance as the frontal solution. Although this solution was not able to stop the CO₂ from accumulating in the entire volume of the CQ, it proved to be efficient in reducing the CO₂ content in the BZ. CO₂ levels at the start of the inhalation in the BZ were three times lower with the lateral PV system installed,

than with just the general ventilation. Numerical capabilities were used in order to study a parameter perhaps more important than the CO₂ content of the BZ: the total quantity of CO₂ inhaled each breath. The results show that the occupant inhaled 8% less CO₂ with the lateral PV solution than without it. Overall, the CFF ventilation circuit coupled with the lateral PV solution achieved the end goal of the thesis: the improvement of air quality in the BZ of the astronauts using the CQ.

The present thesis opens up future research perspectives for the application of PV solutions in confined spaces aboard spacecraft in order to aid the removal of CO_2 from the breathing zone. The PV system should be easy to implement and if possible be passively supplied with air from an existing ventilation circuit so as to not increase energy consumption. Over-reliance on such a system should be avoided, in the sense that it should always be accompanied by a general ventilation circuit. Dust accumulation has proven to be an issue aboard the ISS and depending on the length and diameter of the PV duct, could affect it as well.

Finally, the use of FFTs in delimiting zones influenced by periodic sources of movement warrants further investigation. They can be a useful tool going forward in the investigation of the human breath. The breathing zone delimited in the present thesis is dependent on the shape of the human face, the size of the nostrils and the breathing function — especially the latter's frequency. Repeating the study with different test subjects, and different shapes and faces of the virtual human models could perhaps aid in providing a definite, generally applicable model of a person's breathing zone.

References

- [1] J. Constantinide, H. Najafi, Present state and future of environmental control systems in space, ASHRAE J. 62 (2020) 12–16.
- [2] J.T. James, The headache of carbon dioxide exposures, SAE Tech. Pap. (2007). https://doi.org/10.4271/2007-01-3218.
- [3] C.M. Matty, Overview of Carbon Dioxide Control Issues During International Space Station/Space Shuttle Joint Docked Operations, 40th Int. Conf. Environ. Syst. 2 (2010) 1–9. https://doi.org/10.2514/6.2010-6251.
- [4] NASA, National Aeronautics and Space Administration HUMAN INTEGRATION DESIGN HANDBOOK, Spaceflight (Lond). (2010) 1–27. https://doi.org/NASA/SP-2010-3407.
- [5] R.M. Bagdigian, N. Marshall, S. Flight, International Space Station Environmental Control and Life Support System Mass and Crewtime Utilization In Comparison to a Long Duration Human Space Exploration Mission, (2015).
- [6] S. Fairburn, S. Walker, 'Sleeping With the Stars' The Design of a Personal Crew Quarter for the International Space Station, in: 31st Int. Conf. Environ. Syst., 2001. https://doi.org/10.4271/2001-01-2169.
- [7] J.L. Broyan, M.A. Borrego, J.F. Bahr, International Space Station USOS Crew Quarters Development, 38th Int. Confeence Environ. Syst. (2008). https://doi.org/10.4271/2008-01-2026.
- [8] J. Broyan, D. Welsh, S. Cady, International Space Station Crew Quarters Ventilation and Acoustic Design Implementation, 40th Int. Conf. Environ. Syst. (2010) 1–16. https://doi.org/10.2514/6.2010-6018.
- [9] T.P. Schlesinger, B.R. Rodriguez, International Space Station Crew Quarters On-Orbit Performance and Sustaining Activities, Int. Conf. Environ. Syst. (2013) 1–9. https://doi.org/10.2514/6.2013-3515.
- [10] J.T. James, V.E. Meyers, W. Sipes, R.R. Scully, C.M. Matty, Crew Health and Performance Improvements with Reduced Carbon Dioxide Levels and the Resource Impact to Accomplish Those Reductions, (2011) 1–7.
- [11] D. Law J., Watkins S., Alexander, W.S. Law J., In-Flight Carbon Dioxide Exposures and Related Symptoms: Associations, Susceptibility and Operational Implications, NASA Tech. Rep. (2010) 1–21. https://doi.org/NASA/TP-2010-216126.
- [12] J.L. Broyan Jr, M.A. Borrego, J.F. Bahr, International Space Station United States Operational Segment Crew Quarters On -orbit vs. Design Performance Comparison, SAE Int. J. Aerosp. 4 (2011) 98–107. https://doi.org/10.4271/2009-01-2367.
- [13] EUROPEAN COMMITTEE FOR STANDARDIZATION, En 13779, Management. (2007) 72.
- [14] C. Son, J. Zapata, C. Lin, Investigation of Airflow and Accumulation of Carbon Dioxide in the Service Module Crew Quarters, Int. Conf. Environ. Syst. (2002) 2341. https://doi.org/10.4271/2002-01-2341.

- [15] E.M. Smirnov, N.G. Ivanov, D.S. Telnov, C.H. Son, V.K. Aksamentov, Computational Fluid Dynamics Study of Air Flow Characteristics in the Columbus Module, (2004). https://doi.org/10.4271/2004-01-2500.
- [16] E.M. Smirnov, N.G. Ivanov, D.S. Telnov, C.H. Son, CFD modelling of cabin air ventilation in the international space station: A comparison of RANS and LES data with test measurements for the Columbus module, Int. J. Vent. 5 (2006) 219–227. https://doi.org/10.1080/14733315.2006.11683739.
- [17] C.H. Son, V.K. Aksamentov, E.M. Smirnov, N.G. Ivanov, D.S. Telnov, CFD Modeling for Ventilation: a Method for Reynolds-Averaged Navier-Stokes (RANS) Data Correlation, (2006).
- [18] C.H. Son, N.G. Ivanov, E.M. Smirnov, D.S. Telnov, CFD analysis of node 1 ventilation and carbon dioxide transport for the maximum stowage configuration, 40th Int. Conf. Environ. Syst. ICES 2010. (2010) 1–9. https://www.scopus.com/inward/record.uri?eid=2-s2.0-84880815509&partnerID=40&md5=90d65d3b6de73053631251129e08198a.
- [19] C.H. Son, E.M. Smirnov, N.G. Ivanov, D.S. Telnov, Cfd Modeling of International Space Station and Visiting Spacecraft Ventilation: Evaluation of Design Solutions for Complex on-Orbit Operations, 3 (2011).
- [20] C. Son, N. Ivanov, D. Telnov, E. Smirnov, Integrated Ventilation Modeling for Crew Quarter Airflow, 41st Int. Conf. Environ. Syst. (2011). https://doi.org/doi:10.2514/6.2011-5079.
- [21] F. Parker, R. West, SP-3006 BIOASTRONAUTICS DATA BOOK Second Edition, (n.d.).
- [22] https://tsi.com/products/ventilation-test-instruments/multi-function-ventilation-meters/velocicalc-multi-function-ventilation-meter-9565/, (n.d.).
- [23] T. van Hooff, B. Blocken, T. Defraeye, J. Carmeliet, G.J.F. van Heijst, PIV measurements and analysis of transitional flow in a reduced-scale model: Ventilation by a free plane jet with Coanda effect, Build. Environ. 56 (2012) 301–313. https://doi.org/10.1016/j.buildenv.2012.03.020.
- [24] M.Z.I. Bangalee, J.J. Miau, S.Y. Lin, J.H. Yang, Flow visualization, PIV measurement and CFD calculation for fluid-driven natural cross-ventilation in a scale model, Energy Build. 66 (2013) 306–314. https://doi.org/10.1016/j.enbuild.2013.07.005.
- [25] A. Li, P. Tao, X. Bao, Y. Zhao, PIV measurements of air distribution in a reduced-scale model Ventilation of a busbar corridor in a hydropower station, Int. J. Vent. 12 (2013) 81–98. https://doi.org/10.1080/14733315.2013.11684004.
- [26] E. Szűcs, Fundamental Studies in Engineering Similitude and Modelling, Elsevier, 1980.
- [27] A.K. Melikov, Personalized Ventilation, Indoor Air. 14 (2004) S541–S549. https://doi.org/10.3233/THC-161180.
- [28] Z. Bolashikov, L. Nikolaev, A.K. Melikov, J. Kaczmarczyk, P. Fanger, Personalized ventilation: air terminal devices with high efficiency, in: Proc. Heal. Build., Singapore, 2003: pp. 850–855.
- [29] J. Kaczmarczyk, A. Melikov, Z. Bolashikov, L. Nikolaev, P.O. Fanger, Human response to

- five designs of personalized ventilation, HVAC R Res. 12 (2006) 367–384. https://doi.org/10.1080/10789669.2006.10391184.
- [30] Z.D. Bolashikov, A.K. Melikov, C.M. Velte, K.E. Meyer, Airflow characteristics at the breathing zone of a seated person: Interaction of the free convection flow and an assisting locally supplied flow from below for personalized ventilation application, RoomVent,12th Int. Conf. Air Distrib. Rooms, Trondheim, Norw. (2011) 1–8.
- [31] A.K. Melikov, R. Cermak, O. Kovar, L. Forejt, T.K. (Editor) Wai, S.C. (Editor) Sakhar, D. (Editor) Cheong, Impact of airflow interaction on inhaled air quality and transport of contaminants in rooms with personalized and total volume ventilation, in: Proc. Heal. Build., Singapore, 2003: pp. 592–597.
- [32] A.K. Melikov, R. Cermak, M. Majer, Personalized ventilation: Evaluation of different air terminal devices, Energy Build. 34 (2002) 829–836. https://doi.org/10.1016/S0378-7788(02)00102-0.
- [33] A. Melikov, T. Ivanova, G. Stefanova, Seat headrest-incorporated personalized ventilation: Thermal comfort and inhaled air quality, Build. Environ. 47 (2012) 100–108. https://doi.org/10.1016/j.buildenv.2011.07.013.
- [34] J. Niu, N. Gao, M. Phoebe, Z. Huigang, Experimental study on a chair-based personalized ventilation system, Build. Environ. 42 (2007) 913–925. https://doi.org/10.1016/j.buildenv.2005.10.011.
- [35] AFNOR (Association Française de Normalisation), EN ISO 7730, 2007.
- [36] ASHRAE, Standard 55/2010, n.d.
- [37] Z. Bolashikov, A. Melikov, M. Spilak, I. Nastase, A. Meslem, Improved inhaled air quality at reduced ventilation rate by control of airflow interaction at the breathing zone with lobed jets, HVAC R Res. 20 (2014) 238–250. https://doi.org/10.1080/10789669.2013.864919.
- [38] A.K. Melikov, J. Kaczmarczyk, Air movement and perceived air quality, Build. Environ. 47 (2012) 400–409. https://doi.org/10.1016/j.buildenv.2011.06.017.
- [39] A. Melikov, T. Sakoi, S. Kolencikova, Impact of Air Movement on Eye Symptoms, (2013).
- [40] Z.D. Bolashikov, A.K. Melikov, Methods for air cleaning and protection of building occupants from airborne pathogens, Build. Environ. 44 (2009) 1378–1385. https://doi.org/10.1016/j.buildenv.2008.09.001.
- [41] Z. Bolashikov, A. Melikov, M. Krenek, Control of the free convective flow around the human body for enhanced inhaled air quality: Application to a seat-incorporated personalized ventilation unit, HVAC R Res. 16 (2010) 161–188. https://doi.org/10.1080/10789669.2010.10390899.
- [42] A.K. Melikov, Human body micro-environment: The benefits of controlling airflow interaction, Build. Environ. 91 (2015) 70–77. https://doi.org/10.1016/j.buildenv.2015.04.010.